UNIVERSIDADE D
COIMBRA

Gabriela Lopes Oliveira

ROLE OF THE ADENINE NUCLEOTIDE TRANSLOCATOR 2 IN P19 EMBRYONAL CARCINOMA STEM CELLS MITOCHONDRIAL PROFILE

Dissertação no âmbito do Mestrado em Biologia Celular e Molecular orientada pelo Doutor Ricardo Jorge Fernandes Marques e pelo Professor Doutor António Joaquim Matos Moreno e apresentada ao Departamento de Ciências da Vida da Faculdade de Ciências e Tecnologia da Universidade de Coimbra.

Setembro de 2019

1 2 9 0

FACULDADE DE
CIÊNCIAS E TECNOLOGIA
UNIVERSIDADE D
COIMBRA

Master in Cellular and Molecular Biology

Role of the Adenine Nucleotide Translocator 2 in P19 Embryonal Carcinoma Stem Cells Mitochondrial Profile

Gabriela Lopes Oliveira
Ricardo Marques
António J. Moreno

Coimbra, September 2019

"The important thing is not to stop questioning.

Curiosity has its own reason for existing."

Albert Einstein

This work was performed at the Mitochondrial Toxicology and Experimental Therapeutics (MitoXT) group, at the Center for Neuroscience and Cell Biology of University of Coimbra, Portugal, under the supervision of Dr. Ricardo Marques (CNC, UC) and Dr. António J. Moreno (DCV, UC) and also of the group leader, Dr. Paulo J. Oliveira (CNC, UC).

This work was funded by FEDER - Fundo Europeu de Desenvolvimento Regional funds through the COMPETE 2020 – Operacional Programme for Competitiveness and Internationalisation (POCI), Portugal - 2020, and by FCT - Fundação para a Ciência e a Tecnologia / Ministério da Ciência, Tecnologia e Inovação under project POCI-01-0145-FEDER-016390-Cancel Stem and UID/NEU/04539/2019.

Agradecimentos

A realização desta dissertação de Mestrado nunca teria sido possível sem o apoio e suporte de várias pessoas. Findo um ano de enorme aprendizagem e de muito trabalho, quero desta forma deixar o meu enorme agradecimento a quem esteve presente ao logo destes meses.

Ao meu orientador, Doutor Ricardo Marques, por ter contribuído para o meu crescimento académico ao longo deste ano. Pelos ensinamentos e pela confiança em mim depositada, pela paciência e por me dar margem para arriscar. Foi, sem dúvida, um grande marco neste meu percurso.

Ao Doutor Paulo Oliveira, por me ter dado a oportunidade de trabalhar numa área que tanto gosto. Pela enorme competência científica e pela sua total dedicação enquanto líder deste grupo incrível.

Aos membros do MitoXT, pelo ambiente fantástico que se vive neste laboratório. À malta de mestrado, pela amizade que criámos e pela constante entreajuda, por sentirmos que estávamos todos no mesmo barco. Em especial à Rafaela, à Margarida e à Sara V., a quem devo parte da minha sanidade mental, não só por nos termos apoiado umas às outras nesta fase final da escrita, mas em todos os momentos ao longo deste ano. Aos alunos de doutoramento, aos Pos-Doc e aos técnicos, pela partilha de conhecimento, pela constante disponibilidade em ensinar e pelos momentos de convívio. Foi, sem sombra de dúvida, um enorme privilégio partilhar estes meses convosco.

Às pessoas que o UC-Biotech me deu a conhecer, por tornarem todas as manhãs, horas de almoço, pausas para o café e finais de dia muito melhores. A boa disposição era uma constante e termino este ano de coração cheio!

Aos meus amigos de Coimbra, por terem sempre paciência para me ouvir falar da minha tese e pelos aconselhamentos e dicas ao longo deste ano.

Aos meus amigos de Bolho, em especial à Adriana que me acompanha desde sempre, pelos cafés e por me fazerem descontrair em fazes mais complicadas.

Aos meus amigos de Anadia, pelo constante ambiente de diversão e por entenderem a minha ausência nesta fase.

Aos meus avós, por todo o carinho. Em especial à minha avó Ester que, mesmo com todas as suas limitações, fez sempre questão de estar presente em todos os momentos da minha vida académica e pessoal.

Ao meu irmão, por tudo o que ele representa para mim e pela forte ligação que temos. Sem o saber, ajudou-me imenso nesta fase, sempre com a sua presença tão descontraída e com a boa disposição que o caracteriza.

Aos meus pais, pelo apoio incondicional em todos os momentos da minha vida e por me incentivarem sempre a tentar fazer mais e melhor. Por todos os esforços que fazem por mim e pelo meu irmão e por termos tão presente o sentido de família. Por sempre terem acreditado em mim e por ficarem tão ou mais felizes do que eu pelas minhas vitórias. Sei que, independentemente do que faça no futuro, a presença e amor deles vai ser uma constante na minha vida.

Abstract

Cancer is considered a heterogenous tissue of several cell types, which have different phenotypes, functions and state of differentiation. Cancer stem cells (CSCs) are amongst the group of cells constituting tumors, being characterized by their strong self-renewal and survival properties. Moreover, they are believed to be responsible for driving new tumors formation and to be more resistant to conventional anticancer therapies than the other cells present within the tumor, which makes them clinically relevant. There are several common functional features among cancer cells, known as the hallmarks of cancer, which include the ability that these cells have to remodel their cellular metabolism. Cancer cells, CSCs included, are thought to rely mostly on glycolysis, even in the presence of oxygen, which confers them adaptative advantages. Adenine nucleotide translocator 2 (ANT2), responsible for the ATP uptake into the mitochondria, has been correlated with a higher glycolytic metabolism and are known to be overexpressed in cancer cells. Thus, our aim was to evaluate ANT2 role in cell growth and in the remodeling of mitochondrial metabolism of CSCs. Using P19 embryonal carcinoma stem cells (P19SCs) as a CSCs model, we analyzed ANT2 expression levels comparing them to their differentiated counterparts. Furthermore, ANT2-siRNA was utilized as a tool to inhibit ANT2 translation, in order to evaluate several parameters regarding cell growth, mitochondria remodeling and cellular metabolism. We showed that ANT2 isoform is overexpressed in P19SCs relatively to P19 derived differentiated cells. Upon ANT2 silencing, metabolic activity and cell mass were measured by sulforhodamine B (SRB) and resazurin assays, respectively, and both were decreased after 48 and 72 hours of transfection. Additionally, by measuring oxygen consumption rate (OCR) using Seahorse XF^{e}96 Extracellular Flux Analyzer, we observed a decreased on mitochondrial respiration after 48 hours of transfection, which was not accompanied by a decreased on mitochondrial

content, since TOM20 protein levels and mitochondrial network area were not affected. Mitochondrial membrane potential was evaluated by fluorescence microscopy imaging using Tetramethylrhodamine methyl ester (TMRM), with silenced cells presenting more depolarized mitochondria. Metabolic-related enzymes, mitochondrial dynamics and biogenesis were evaluated by Western blotting and no differences were found in pyruvate kinase muscle isozyme M2 (PKM2), mitofusin 1 (MFN1) and dynamin-related protein-1 (DRP1) expression levels, however, hexokinase II (HKII), Pyruvate dehydrogenase kinase (PDK), Peroxisome proliferator-activated receptor-gamma coactivator 1-alpha (PGC-1-α) and Mitochondrial transcription factor A (TFAM) were decreased after ANT2 silencing.

Our findings demonstrate that ANT2 is more expressed in P19SCS when compared to their differentiated counterparts. Additionally, ANT2 silencing seems to promote a decrease in cell growth and a metabolic adaptation in CSCs towards a less oxidative phenotype, although having the same amount of mitochondria. Albeit mitochondrial dynamics seemed not to be affected, mitochondrial biogenesis was decreased by around 25% upon ANT2 silencing. Based on our data and on the increasing evidence that ANT2 plays a role in the metabolic remodeling of CSCs, ANT2 could be a promising metabolic target for anticancer therapy against CSCs.

Keywords: Adenine nucleotide translocator 2; cancer stem cells; mitochondria; metabolic remodeling

Resumo

O cancro é considerado um tecido heterogéneo composto por vários tipos de células, que possuem diferentes fenótipos, funções e estados de diferenciação. As células estaminais cancerígenas (CSCs) estão entre o grupo de células que constituem os tumores, sendo caracterizadas pelas suas fortes propriedades de autorrenovação e sobrevivência. Além disso, acredita-se que sejam responsáveis pela formação de novos tumores e serem mais resistentes às terapias anticancerígenas convencionais do que as restantes células presentes no tumor, o que as torna clinicamente relevantes. Existem várias características funcionais comuns entre as células cancerígenas, conhecidas como os *hallmarks* do cancro, que incluem a capacidade que estas células têm de remodelar o seu metabolismo celular. Acredita-se que as células cancerígenas, incluindo as CSCs, dependam principalmente da glicólise, mesmo na presença de oxigênio, o que lhes confere vantagens adaptativas. O transportador de nucleotídeos de adenina 2 (ANT2), responsável pela importação de ATP para a matriz mitocondrial, tem sido correlacionado com um metabolismo glicolítico mais elevado e sabe-se que é sobre expresso em células cancerígenas. Assim, o nosso objetivo foi avaliar o papel do ANT2 na proliferação celular e na remodelação do perfil mitocondrial, bem como no metabolismo das CSCs. Usando as células P19 estaminais de carcinoma embrionário (P19SCs) como modelo de CSCs, analisámos os níveis de expressão de ANT2 comparativamente com suas contrapartes diferenciadas (P19dCs). Além disso, ANT2-siRNA foi utilizado como ferramenta para inibir a tradução de ANT2, a fim de avaliar vários parâmetros em relação ao crescimento celular, remodelação mitocondrial e metabolismo celular. Neste trabalho demonstramos que a isoforma ANT2 é sobre expressa em P19SCs relativamente às P19dCs. Após o silenciamento do ANT2, a atividade metabólica e a massa celular foram medidas usando sulforrodamina B (SRB) e resazurina, respetivamente, e ambos diminuíram após 48 e 72 horas de transfeção. Além

disso, medindo a taxa de consumo de oxigénio (OCR) usando Seahorse XFe96 Extracellular Flux Analyser, observámos uma diminuição na respiração mitocondrial após 48 horas de transfeção, o que não foi acompanhado por uma diminuição no conteúdo mitocondrial, uma vez que os níveis proteicos de TOM20 e a área da rede mitocondrial não foram afetados. O potencial de membrana mitocondrial foi avaliado por microscopia de fluorescência usando metil éster de tetrametilrodamina (TMRM), sendo possível observar que as células silenciadas apresentam mitocôndrias mais despolarizadas. Dinâmica e biogénese mitocondrial, e enzimas relacionadas com o metabolismo foram avaliadas por Western blotting e não foram encontradas diferenças nos níveis de expressão de isoenzima piruvato cinase M2 (PKM2), mitofusina 1 (MFN1) e proteína relacionada à dinamina 1 (DRP1) mas, no entanto, hexocinase II (HKII), piruvato desidrogenase cinase (PDK), coativador do receptor-gama ativado por proliferador de peroxissoma 1-alfa (PGC-1-α) e fator de transcrição mitocondrial A (TFAM) diminuíram após o silenciamento do ANT2.

Os nossos resultados demonstram que o ANT2 é mais expresso nas P19SCS do que nas P19dCs. Adicionalmente, o silenciamento de ANT2 parece promover uma diminuição no crescimento celular e uma adaptação metabólica nas CSCs para um fenótipo menos oxidativo, embora tenham a mesma quantidade de mitocôndrias. Ainda que a dinâmica mitocondrial pareça não ter sido afetada, a biogénese mitocondrial apresenta uma diminuição de cerca de 25% com o silenciamento do ANT2. Com base nos nossos dados e na crescente evidência de que o ANT2 desempenha um papel na remodelação metabólica das CSCs, o ANT2 poderá ser um alvo metabólico promissor para a terapia anticancerígena de CSCs.

Palavras-chave: Transportador de nucleótidos de adenina 2, células estaminais cancerígenas, mitocôndria, remodelação metabólica

List of Acronyms and Abbreviations

Acetyl-CoA	Acetyl coenzyme A
ADP	Adenosine diphosphate
AMP	AMP-activated Protein
AMPK	AMP-activated Protein Kinase
ANT	Adenine nucleotide translocator
APS	Ammonium persulfate
ATP	Adenosine triphosphate
BCA	Bicinchoninic acid
BSA	Bovine serum albumin
CO_2	Carbon dioxide
CSC	Cancer stem cell
CyP-D	Cyclophilin D
DMEM	Dulbecco's modified eagle's medium
DMSO	Dimethyl sulfoxide
DNA	Deoxyribonucleic acid
DRP1	Dynamin-related protein-1
DTT	Dithiothreitol
ECAR	Extracellular acidification rate
EDTA	Ethylenediaminetetraacetic acid
ETC	Electron transport chain
$FADH_2$	Flavin adenine dinucleotide
FBS	Fetal bovine serum
FH	Fumarate hydratase
GLS	Glutaminase
GLUT	Glucose transport proteins
HCl	Hydrogen chloride
HK	Hexokinase
HRP	Horseradish peroxidase

IMM	Inner mitochondrial membrane
LDH	Lactate dehydrogenase
MCT	Monocarboxylate transporters
MFN	Mitofusin
MOMP	Mitochondrial outer membrane permeabilization
mPTP	Mitochondrial permeability transition pore
mRNA	Messenger RNA
mtDNA	Mitochondrial DNA
NADH	Nicotinamide adenine nucleotide (reduced form)
NADPH	Nicotinamide adenine nucleotide phosphate (reduced form)
NaOH	Sodium hydroxide
OCR	Oxygen consumption rate
OCT4	Octamer-binding transcription factor
OMM	Outer mitochondrial membrane
OPA1	Optic atrophy-1
OXPHOS	Oxidative phosphorylation
PBS	Phosphate buffered saline
PDH	Pyruvate dehydrogenase
PDK	Pyruvate dehydrogenase kinase
PFK	Phosphofructokinase
PGC-1-α	Peroxisome proliferator-activated receptor-gamma coactivator 1-alpha
PKM2	Pyruvate kinase muscle isozyme M2
PMSF	Phenylmethanesulfonyl fluoride
PPP	Pentose phosphate pathway
PVDF	Polyvinylidene difluoride
RA	Retinoic acid
RNA	Ribonucleic acid
ROS	Reactive oxygen species
SDH	Succinate dehydrogenase
SDS	Sodium dodecyl sulphate
SDS-Page	Sodium dodecyl sulfate polyacrylamide gel

SEM	Standard error of the mean
siRNA	Small-interfering RNA
SRB	Sulforhodamine B
TBS-T	Tris-buffered saline tween
TCA	Trichloroacetic acid
TEMED	N,n,n′,n′-tetramethylethylenediamine
TFAM	Mitochondrial transcription factor A
TMRM	Tetramethylrhodamine methyl ester
TOM20	Translocase of outer membrane 20
TROMA-I	Trophectodermal cytokeratin 8 Endo-A
UV	Ultraviolet
VDAC	Voltage-dependent anion channel

List of Content

Figures Index

Tables Index

1. Introduction

1.1. Cancer: an overview

According to the World Health Organization, cancer was responsible for 8.8 million deaths in 2015, being the second leading cause of death worldwide. Cancer can be defined as a set of diseases in which a group of abnormal cells acquires the ability to grow in an uncontrolled way by disregarding the normal rules of cell division. Unlike healthy cells, cancer cells bypass death signals and continue to grow, potentially spreading from the tissue of origin to other tissues throughout the body through a process called metastasis.

Cancer development is a complex multi-step process that involves the acquisition of functional and genetic abnormalities. The origins of cancer are multifactorial and influenced by exogenous (tobacco, chemicals, radiations, and infectious organisms) and endogenous (hormones, immune conditions, inherited mutations and metabolic alterations) factors.

Tumors are complex tissues, meaning that they are heterogeneous and composed of different cell types and subtypes, including immune inflammatory cells, fibroblasts, cancer stem cells, among others (1) (Fig. 1). Collectively, those cells allow tumor growth and progression. Therefore, the individual study of the different cell types present within a tumor is needed in order to understand tumor biology as a whole.

In 2000, Hanahan and Weinberg (2) recognized six common functional features shared by most cancer cells that allow them to survive, proliferate, and disseminate. These properties, known as the hallmarks of cancer, include the following biological capabilities: resisting cell death, sustaining proliferative signaling, inducing angiogenesis, evading growth suppressors, enabling replicative immortality, and activating invasion and metastasis. More recently, in 2011 (1), these properties were re-evaluated and four more were added:

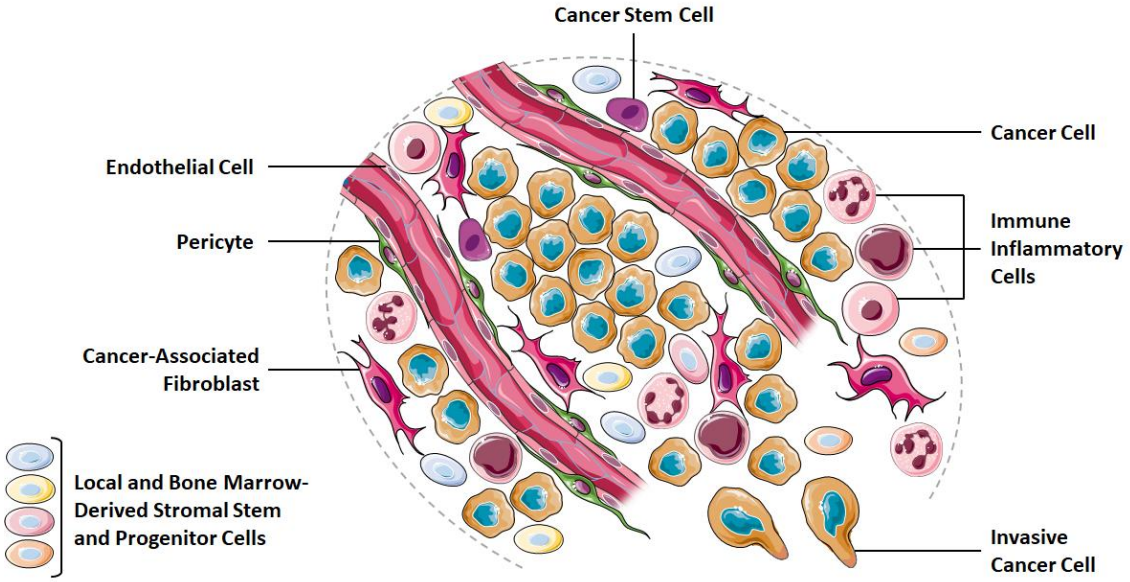

Figure 1 - Tumor heterogeneity. Most solid tumor tumors are constituted by an assemblage of distinct cell types known to contribute to the biology of the tumor. Within a tumor are present cells from the immune system, fibroblasts, endothelial cells, cancer stem cells, among others.

"deregulating cellular energetic" and "avoiding immune destruction" as emerging hallmarks; and "genome instability and mutations" and "tumor-promoting inflammation" as enabling hallmarks. These 10 features are considered crucial properties that help to understand the complexity of cancer.

As mentioned before, one of the emerging hallmarks is the deregulation of cellular metabolism. Although normal cells acquired nutrients in a regulated way by stimulation of growth factors, cancer cells are able to overcome this dependence. Cancer cells do so by acquiring mutations, which ultimately leads to alterations in signaling pathways. Increasing evidence has been showing that some of these pathways are involved in nutrients uptake (3) and metabolism (4), fueling cell growth and proliferation, and promoting cell survival (5).

1.1.1. Deregulating cellular bioenergetics

There are two major processes by which mammalian cells obtain energy: 1) via glycolysis and 2) via oxidative phosphorylation (OXPHOS). During

glycolysis, a process that occurs in the cytosol, glucose is metabolized to two molecules of pyruvate, generating two net molecules of ATP and two NADH molecules. OXPHOS, the second pathway to produce energy, occurs mainly in mitochondria in an oxygen-dependent way. After glucose being metabolized to pyruvate via glycolysis, pyruvate is converted to Acetyl-CoA by pyruvate dehydrogenase (PDH) and enters into the Krebs cycle in order to be completely oxidized to carbon dioxide, generating energy and reducing power (ATP, NADH and the reduction of $FADH_2$ in Complex II by succinate generated in the cycle). The reducing equivalents generated are then used by the mitochondrial electron transport chain (ETC) to synthesize ATP via OXPHOS. The electrons released by NADH and succinate oxidation flow along the electron transport chain to oxygen, via protein complexes located in the inner membrane. This electron flux allows the pumping of protons out of the mitochondrial matrix to the intermembrane space, creating a proton motive force which is composed by the transmembrane electrical potential and the gradient of proton concentration (6). Then, through an enzyme complex known as complex V or ATP-synthase, protons reenter to the mitochondrial matrix, which leads to the formation of, approximately, 32 ATP molecules. As OXPHOS is more efficient than glycolysis to generate ATP, non-proliferative cells rely mostly on OXPHOS when oxygen is present. Because oxygen is required as the final electron acceptor in this process, when it is not present, cells can redirect the pyruvate formed via glycolysis generating lactic acid by lactate dehydrogenase A (LDHA), a process known as "anaerobic glycolysis" (7).

The energy metabolism of most cancer cells differs from normal cells. In the 1920s, Otto Warburg, a pioneer in the study of respiration, made an interesting discovery in cancer metabolism: even in the presence of oxygen, many types of cancer cells prefer to metabolize glucose to lactate, and exhibited higher levels of glucose uptake when compared to normal cells (8, 9, 10). This switch from OXPHOS to glycolysis is known as "aerobic glycolysis" or "Warburg

effect". To justify this metabolic remodeling, Warburg proposed that, in tumors, mitochondria are decreased or functionally impaired, which leads to impaired aerobic respiration (10). However, subsequent studies showed that, in fact, proliferating lymphocytes also rely on glycolysis (11, 12), suggesting that this metabolic pattern is not unique to cancer cells, and being an evidence that damaged OXPHOS could not be the cause of the switch to aerobic glycolysis. In addition, other studies showed that OXPHOS is not impaired or decreased in highly proliferative tumor cell lines (13, 14).

Interestingly, even when tumors are well vascularized and oxygen is available in higher amounts, cancer cells still prefer to use aerobic glycolysis, suggesting that glycolysis provides an advantage to them beyond ATP generation in the absence of oxygen (15).

1.1.1.1. Metabolic reprogramming: a selective advantage in cancer cells

Cancer cells are characterized by having an increased division rate. Because of that, they have high needs for energy, nutrients, and biosynthetic activity so they can have enough macromolecular components to divide and proliferate. Thus, cancer cells can readapt their metabolism, acquiring a different metabolic profile when compared to normal cells (Fig. 2). Many reports have highlighted the benefits of favoring glycolysis over mitochondrial oxidation. Using glycolysis, cells can generate ATP more rapidly than using OXPHOS (16), which is suited to the energy demands that tumor cells need to proliferate. Also, increased transcription of glycolytic enzymes (13, 17), expression of alternate hexokinase isoforms (18) and increased expression of glucose transporters (19), are common features found in cancer cells. These alterations ultimately lead to increased intracellular levels of glucose, thus stimulating glycolysis.

Another important characteristic of the Warburg effect is that the high rates of glycolysis promote the accumulation of lactate in the intracellular space. Lactate production by LDHA allows the regeneration of NAD+, which is essential for glycolysis to continue. Lactate, together with H^+, are then secreted to the microenvironment via the monocarboxylate transporters (MCT), which results in a decreased pH of the extracellular environment (20). It has been demonstrated that in some types of cancer, such as neuroblastoma and colorectal carcinoma, MCT1 and MCT4 expression levels are increased, which has also been associated with a poor prognosis (21, 22). Furthermore, several studies suggest that acidification of extracellular environment may contribute to oncogenesis, leading to increased activity of pro-invasion factors and stimulating tumor cell invasion, angiogenesis, and metastasis (23, 24, 25).

Additionally, Bellance et al. (26) suggest that increased glycolysis generates the carbon intermediates required for various biosynthetic pathways, which facilitates the biosynthesis of the macromolecules and organelles required for assembling new cells (1). Thus, large amounts of lipid and nucleotide precursors are needed to maintain their uncontrolled growth proliferation. Lipids are used to form cell membranes and energy storage, and nucleotides to DNA replication (27). Because cancer cells need to generate those components in a rapid way, the pentose phosphate pathway (PPP) also plays an important role in their metabolism. Thus, as glycolysis is directly connected to the PPP, cancer cells can generate ribose-5-phosphate, contributing to the synthesis of macromolecules, and NADPH, an essential reductant in anabolic processes (28). It was found that PPP is upregulated in many types of tumors (29, 30), and it is involved in apoptosis avoidance by facilitating DNA damage repair and by protecting cells from oxidative stress (27).

Besides having an increased glucose uptake and metabolism, another metabolic feature that many cancer cells have is a dependence on glutamine uptake and metabolism (31). Glutamine can be used as a precursor for the

synthesis of amino acids, nucleotides, proteins, and lipids, which are needed to cell growth and proliferation. Once internalized by the cell, glutamine is converted to glutamate by mitochondrial glutaminase (GLS) and then, in the

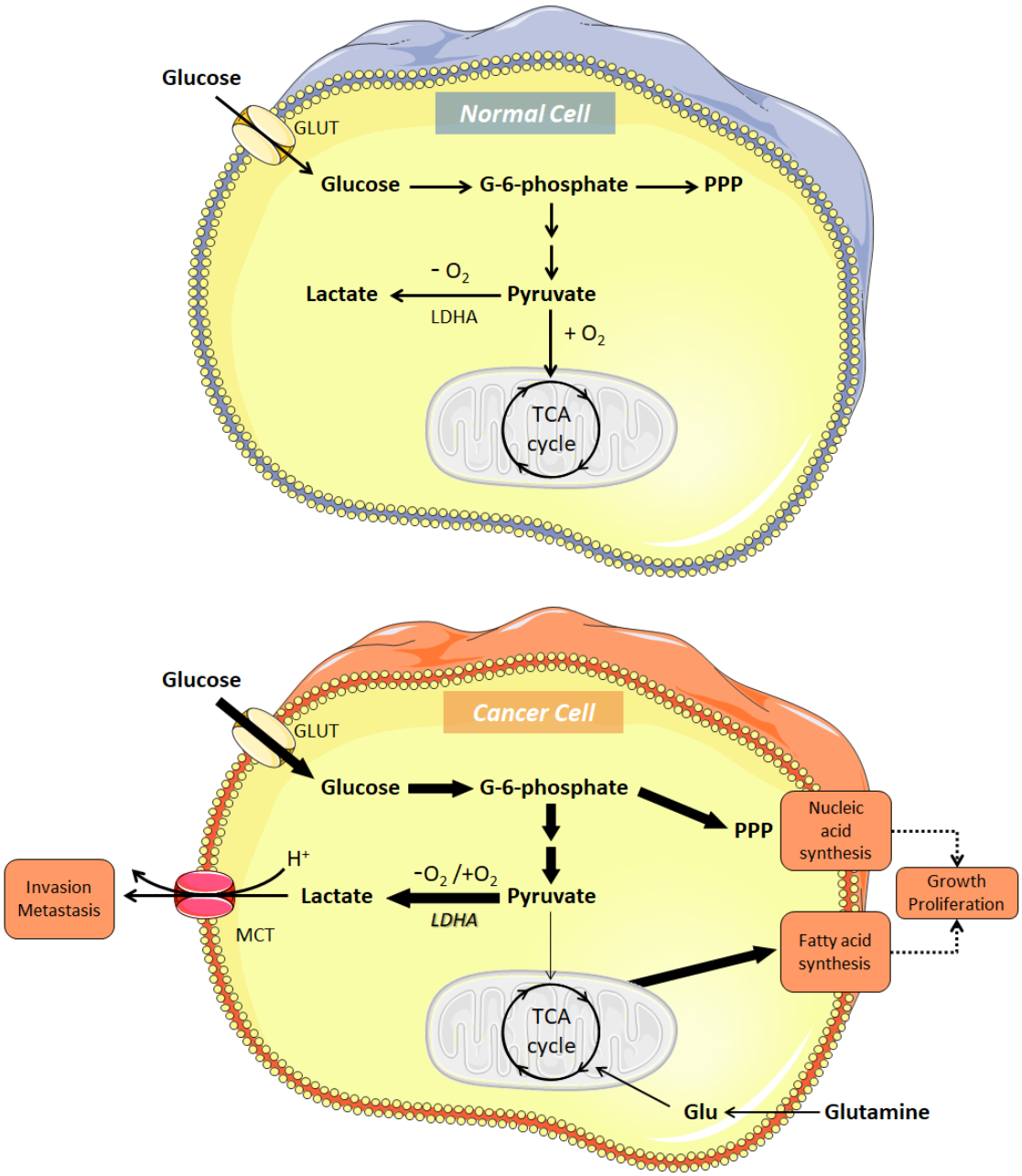

Figure 2 - Metabolic differences between normal and cancer cells. In normal cells, when O_2 is present, glucose is metabolized to pyruvate which is oxidized to CO_2 through the TCA cycle. Only if O_2 is limited, pyruvate is metabolized to lactate. Cancer cells, even in the presence of oxygen, mostly rely on glycolysis, generating lactate. When secreted to the microenvironment, lactate favors tumor progression. Aerobic glycolysis also allows the generation of metabolic intermediates for macromolecular biosynthesis, promoting cell growth and proliferation. Moreover, glutamine also serves as a substrate to fuel the TCA cycle. Glu: Glutamate; GLUT: Glucose transporter; LDHA: Lactate dehydrogenase A; MCT: Monocarboxylate transporter; PPP: Pentose phosphate pathway.

TCA cycle, is metabolized to α-ketoglutarate. This process, known as glutaminolysis, is considered an alternative fuel bioenergetic pathway. Furthermore, glutamine can also be metabolized into pyruvate by malic enzyme, and then to lactate by LDH, which will lead to the production of NADPH and NADH, respectively (7).

Thus, in cancer cells, both glucose and glutamine are important carbon sources for the generation of energy and anabolic precursors. Also, the ability that cancer cells have to remodel their own metabolism, gives them several advantages, promoting their survival and tumor progression.

1.1.1.2. Mechanisms involved in metabolic reprogramming

Several studies have suggested that the Warburg effect is more closely related to alterations in signaling pathways than to mitochondrial defects. Warburg effect has been explained by some molecular mechanisms involving oncogenes (AKT, MYC, and RAS), tumor suppressor genes (AMPK, P53, succinate dehydrogenase and fumarate hydratase), and the hypoxia-inducible factor (HIF-1) pathway (32) (Fig. 3).

The PI3K/AKT pathway is one of the most commonly activated oncogenic signaling pathways in tumors, having a central role in regulating cell proliferation and survival (33), cancer cell invasion (34), and also cancer metabolism (35, 36). The best-known effector downstream of PI3K is AKT, which can stimulate glycolysis by increasing expression and membrane translocation of glucose transporters (GLUT1, GLUT2, and GLUT4) and by phosphorylating key glycolytic enzymes (37, 38). Akt activation can also stimulate hexokinase 1 (HK1), hexokinase (HK2) and phosphofructokinase (PFK) activities and is also able to activate the hypoxia-inducible factor 1 (HIF-1). As a result, HIF-1 potentiates, even more, the enhancement of glycolysis, by upregulating glucose transporters

(GLUT1, GLUT3), glycolytic enzymes (HK1, HK2, LDHA, among others) and monocarboxylate transporter 4 (MCT4), which transports lactate out of the cell. Furthermore, it also activates pyruvate dehydrogenase kinase (PDK) (39), a negative regulator of pyruvate dehydrogenase (PDH). PDH is the enzyme responsible for converting pyruvate into acetyl-CoA to enter the Krebs cycle in the mitochondria. Thus, its inhibition leads to the diversion of pyruvate from the mitochondria, decreasing mitochondrial respiration. Moreover, the oncogene MYC also cooperates with HIF-1 and induces most of the glycolytic genes mentioned above (40). MYC also plays a role in glutamine metabolism, regulating the expression of mitochondrial glutaminase 1 (GLS1) and promoting

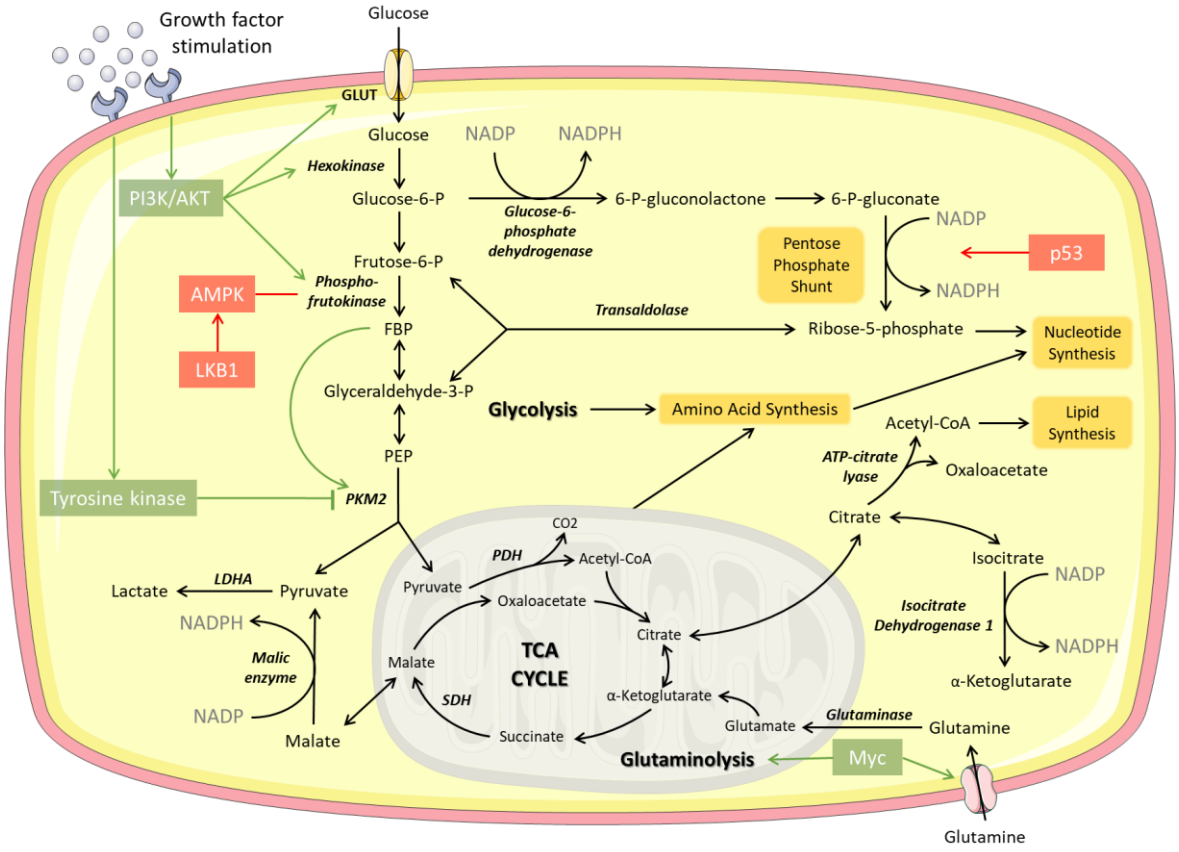

Figure 3 - Oncogenes and tumor suppressors and their role in cancer metabolism. The signaling pathways of both oncogenes and tumor suppressor genes control the metabolic pathways of cancer cells. Growths factors lead to the activation of PI3K/Akt, that increases the uptake of glucose and the activity of glycolytic enzymes, which stimulate glycolysis. Myc stimulates glutaminolysis, supporting NADPH production and lipid synthesis. Tumor suppressors p53 and AMPK decrease metabolic flux through glycolysis in response to cell stress. Oncogenes are represented in green and tumor suppressors in red. FBP: fructose 1,6-bisphosphate; GLUT: Glucose transporter; LDHA: Lactate Dehydrogenase A; PDH: Pyruvate Dehydrogenase; PEP: Phosphoenolpyruvate; SDH: Succinate Dehydrogenase.

the transport of glutamine inside the cell by increasing the expression of the glutamine transporters (41).

Tumor suppressor genes code for proteins that normally operate to restrict cellular growth and division, repair DNA mistakes and also promote programmed cell death (apoptosis). They are usually silenced in cancer, which can promote cells to grow in an uncontrolled way. For instance, p53 plays an important role as a defense mechanism against tumor development, being involved in the regulation of apoptosis, DNA repair mechanisms, among others (42). It is also involved in metabolic stress response, promoting OXPHOS and inhibiting glycolysis in normal conditions. p53 is involved in the inhibition of GLUT1 and GLUT2 transcription, and is also responsible for the upregulation of TIGAR, an apoptosis regulator that decreases the levels of fructose-2,6-bisphosphate (32, 43). Another tumor suppressor gene that also has an important role in metabolic remodeling is AMP-activated protein kinase (AMPK). AMPK is activated under stress conditions, such as nutrient deprivation and hypoxia, and functions as a cellular sensor of AMP. AMPK promotes OXPHOS and inhibits proliferation when the ratio of AMP/ATP is high (44).

Succinate dehydrogenase (SDH) and fumarate hydratase (FH) are enzymes involved in the Krebs cycle, being responsible for the conversion of succinate to fumarate and fumarate to malate, respectively. SDH is also a functional member (complex II) of the electron transport chain (ETC) (45). Several studies identified them both as tumor suppressors, and oncogenic mutations lead to the accumulation of their substrates (45, 46). The increase in the levels of succinate and fumarate induces a pseudo-hypoxic response and leads to glycolytic enzymes activation, through inhibition of HIF degradation (44).

Thus, mutations that interfere with oncogenes and/or tumor suppressor genes and their signaling pathways promote alterations in cell metabolism, leading to the Warburg effect.

1.1.1.3. Mitochondria and cancer

Although tumor cells rely mainly on glycolysis, mitochondria remain essential for cancer progression. Besides their function as ATP producers, mitochondria also play important roles in cell death regulation, in generating reactive oxygen species (ROS), in the biosynthetic metabolism, among others (47). However, mitochondrial biology of cancer cells has significant differences when compared to normal cells, which leads to alterations in their functional properties.

Mitochondria are known to be dynamic organelles, meaning that they can alter their morphology according to their needs by fusion and fission processes (48). The cell energetic state is often associated with specific mitochondrial morphologies (49). Furthermore, mitochondrial shape also affects susceptibility to apoptosis and mitophagy (47, 48). In mammalian cells, some of the proteins involved in mitochondrial fission are dynamin-related protein-1 (DRP1) and fission protein 1 (FIS1); and, on the order hand, optic atrophy-1 (OPA1), mitofusin 1 (MFN1) and mitofusin 2 (MFN2) are associated with mitochondrial fusion (50). Several studies suggest that an increased OXPHOS activity (and its consequent ATP generation) is correlated with elongation of mitochondria, having a more tubular network (44, 45); thus, it is thought that this mitochondrial morphology is more efficient not only for ATP production, but also for distributing energy through long distances (46, 51).

It has been demonstrated that, in cancer cells, there is an imbalance of fusion and fission activities, which ultimately results in a fragmented mitochondrial network (52). Examples of alterations that are known to be present in some tumor cells are an enhanced DRP1 activity and/or downregulation of MFN2, which were found in several cancer types like lung cancer (53), breast cancer (54), among others (52), resulting in more inactive mitochondria. Thus, these results suggest that a more glycolytic phenotype is accompanied by a less

elongated mitochondrial network, with cells presenting smaller and fragmented mitochondria.

Mitochondrial permeability transition pore (mPTP) is a dynamic molecular complex that also is known to play an important role in cancer cells. Despite some controversial opinions about its role and its constituents, it is thought to be composed by the voltage-dependent anion channel (VDAC) in the outer mitochondrial membrane (OMM), the adenine nucleotide translocator (ANT) in the inner mitochondrial membrane (IMM), cyclophilin D (CyP-D) and some other proteins such as hexokinase (HK) (55). mPTP is known to be involved in apoptosis regulation in a complex process regulated at multiple steps (56). Mitochondrial outer membrane permeabilization (MOMP), upon the opening of the mPTP, which is triggered by elevated matrix [Ca^{2+}], leads to the release of pro-apoptotic proteins from the mitochondrial intermembrane space, that are responsible for the initiation of the apoptotic event. This mechanism involves the release of cytochrome C from mitochondria and caspase activation (57). In addition, several studies showed that increased ROS levels and mitochondrial depolarization are some of the sensitizing factors that lead to mPTP opening (58). It is also described that cancer cells have a more polarized mitochondrial membrane potential ($\Delta\Psi m$) than normal cells, which is also correlated with the malignancy of the cells, meaning that the more polarized $\Delta\Psi m$ is, the more aggressive is the cell (59). Besides that, it was also demonstrated that in cancer cells mitochondria is related to a decreased apoptosis rate, helping cells to grow and proliferate (60).

Furthermore, mutations and alterations in the number of copies of mitochondrial DNA (mtDNA), that is essential to encode several proteins related to mitochondrial respiration, are being correlated with cancer (61).

1.2. Tumor heterogeneity and cancer stem cells

Tumors are complex tissues composed of different types of cancer cells that have different phenotypes, different states of differentiation and different functions (Fig. 1). There are two different models that try to explain this tumor heterogeneity: the stochastic model and the hierarchy model. The first theory, also called clonal evolution, suggests that tumor heterogeneity arises from different genetic hits affecting different cells that were originated from the same initial cell (62), and every single cell can self-renew and propagate tumors. In contrast, the hierarchy model, also known as cancer stem cell (CSC) model, suggests that a small subpopulation of cells within the tumor are able to self-renewal and differentiate into a variety of cell types, with different abilities and phenotypes (63, 64). In addition, equivalent to what happens in a normal tissue supported by healthy stem cells, tumors are organized in a hierarchy of heterogeneous cell populations as a result of the process of differentiation (65). Therefore, CSCs are thought to be the source of tumor heterogeneity and initiation (66). Although there are different models to explain tumor heterogeneity, in fact, they are not mutually exclusive. For instance, it was shown that leukemic CSCs undergo clonal evolution (67).

Evidence for CSCs was first observed in hematological malignancies, where only a small subpopulation of cancer cells was capable of forming new tumors when transplanted to immunocompromised mice (68). Subsequent studies were done in solid tumors, as breast (69) and brain (70) cancer among others (71, 72), supporting the idea of tumor heterogeneity, and suggesting the hypothesis of CSCs as tumor-initiating cells. The exact origin of CSC is still unclear, but it is thought that mutation hits may occur and accumulate in proliferating stem cells, progenitor cells, and even differentiated somatic cells (73).

However, despite some features regarding CSCs biology and their metabolism were already been studied, much is still unknown about this

important tumor cell subtype, their underlying mechanisms and how to properly target them.

1.2.1. Cancer stem cells and resistance to therapy

The definition of CSC was established as "a cell within a tumor that possesses the capacity to self-renew and to cause the heterogeneous lineages of cancer cells that comprise the tumor" (74). CSCs have similarities with normal stem cells, meaning that they have features in common. Like stem cells, CSCs have the ability to divide symmetrically, forming identical daughter stem cells that retain self-renewal capacity; or asymmetrical, giving rise to one stem cell and one more differentiated progenitor cell.

CSCs also have other properties that allow them to have a long lifespan, such as enhanced DNA repair mechanisms, quiescence state, upregulated expression of several drug transporters, high expression of anti-apoptotic proteins, among others (75).

Conventional chemotherapies and radiotherapies target proliferating cells and require active cycling for induction of apoptosis. As CSCs are known to be quiescent or slow-cycling compared with their differentiated counterparts, they are not targeted by conventional therapies, meaning that they are resistant to those therapies and are able to survive. Moreover, it was shown that cancer relapse after chemotherapy treatments often leads to the formation of a more aggressive tumor than the original one, because of the selection pressures introduced by drug administration (76).

CSCs have several self-protection mechanisms that allow them to avoid being targeted by conventional therapies, such as increased levels of anti-apoptotic proteins (77), enhanced DNA repair mechanisms (78) and overexpression of ATP-binding cassette (ABC) transporters (79). ABC transporters are transmembrane proteins that function as active transporters,

mediating the transport of substrates against the concentration gradient. They are shown to be involved in the transport of chemotherapy drugs out of the cell (79), as well as cell-signaling molecules that contribute to tumorigenesis (80), but their underlying mechanism and other possible roles are not totally understood (81). Furthermore, CSCs also present decreased concentrations of ROS and more active ROS defenses when compared to their non-tumorigenic progeny, which also is related with cancer resistance (82), avoiding DNA damage (75) and sustaining stem-like properties (83).

Thus, because of the capacity that CSCs have to avoid conventional therapies and their involvement in cancer resistance, more studies in this field need to be done in order to better understand their underlying mechanisms and to identify possible targets to kill CSCs and overcome cancer relapse.

1.2.2. The metabolic profile of cancer stem cells

As explained in the previous sections, metabolic remodeling is considered one of the hallmarks of cancer and, in the majority of tumors, cancer cells rely preferably on glycolysis instead of OXPHOS. CSCs demonstrate unique metabolic flexibility, with many reports suggesting that they can be more glycolytic or more oxidative in a type-dependent manner (84).

Several studies performed in some cancer types suggest that CSCs have a stronger glycolytic phenotype when compared with differentiated cancer cells (85, 86). Furthermore, CSCs also showed to have a decreased PDH expression, and increased expression of glycolytic enzymes (HKII and PDK), glucose uptake (GLUT1), lactate synthesis and ATP content together with a decreased mitochondrial function (86, 87, 88). Besides that, further reports revealed that stimulation of glycolysis is necessary for cell immortalization and is sufficient to increase cellular lifespan (89). Together, these features suggest that CSCs have

distinct metabolic profiles in comparison to non-CSCs and to their differentiated counterparts, being more glycolytic.

In contrast, other publications showed that, in other cancer types, CSCs had demonstrated a preference for OXPHOS to energy production. They showed an increased mitochondrial mass, combined with enhanced mitochondrial ROS, higher rates of oxygen consumption, increased membrane potential and overall increased mitochondrial function (90, 91).

It is important to mention that, because of the ability that CSCs have to readapt and alter their metabolism according to the microenvironment, it was suggested that futures therapies must target both glycolysis and OXPHOS (92).

Collectively, those findings evidence the apparent heterogeneity and plasticity of CSCs regarding their metabolic profiles, which allow them to survive even under conditions of stress.

1.2.2.1. Mitochondria in cancer stem cells

CSCs, similarly to their differentiated counterparts, have also been described to have alterations in mitochondrial biology and physiology (92).

Regarding CSCs that have a glycolytic phenotype and their mitochondria dynamic events, studies with DRP1, a protein known to be involved in mitochondrial fission, showed that fission can play a role in stemness maintenance (93); and inhibition of DRP1 promoted apoptosis and inhibited CSCs growth in glioblastoma (94). Furthermore, peroxisome proliferator-activated receptor-gamma coactivator 1-alpha (PGC-1-α), a mitochondrial biogenesis mediator, is thought to be downregulated in CSCs, in analogy with normal stem cells, that only overexpressed PGC-1-α during differentiation (92).

Vega-Naredo et al. (86), by using an embryonal carcinoma stem cell model (P19), showed that differentiation of CSCs occurs in association with a mitochondrial remodeling. It was observed that, when compared to their

differentiated counterparts, P19 stem cells (P19SC) have a stronger glycolytic phenotype, showing more undeveloped and fragmented mitochondria, with a lower $\Delta\Psi m$ and also a more closed mPTP conformation. In contrast, their differentiated counterparts (P19dCs) are more oxidative, albeit still being glycolytic, and presented more elongated and more polarized mitochondria. Another interesting result was that ANT levels were different between both P19SCs and P19dCs (more detail in section 3).

In CSCs with an oxidative phenotype, several studies were done regarding their mitochondria biogenesis. Peroxisome proliferator-activated receptor-gamma coactivator 1-alpha (PGC-1-α), a mitochondrial biogenesis mediator, is increased in a subset of human melanoma tumors (95) and in circulating tumor cells (96). Furthermore, PGC-1α inhibition in breast CSCs reduced the stemness properties (97). These findings support the idea that mitochondrial biogenesis plays an important role in CSCs maintenance. Moreover, it has been demonstrated that overproduction of mitochondrial ROS, inhibition of mitochondrial biogenesis and reduction of mitochondrial potential affect the capacities of proliferation and survival in CSCs (98, 99).

Thus, taking into account that mitochondria from CSCs are not identical to the more differentiated tumor cells, mitochondrial biology and physiology are believed to be a good target for cancer therapy, because they are fundamental in CSCs maintenance.

1.3. Adenine nucleotide translocator

The most abundant protein in mitochondria, ANT, is a mitochondrial protein located in the inner membrane (100) and has a major physiological role in the exchange of ADP/ATP across the inner membrane but also is thought to be part of mPTP. It comprises 300–320 amino acid residues forming six transmembrane

helices and its functional unit is a homodimer that acts as a gated pore channeling single molecule of ADP and ATP (55). In normal conditions, when mitochondrial respiration is working properly, it drives to the formation of $\Delta\Psi m$ across the mitochondrial inner membrane, which in turns is used to generate ATP via ATP synthase (also known as complex V). Then, ATP is exported to the cytosol, where it is most needed to maintain cell functions, in exchange for ADP by ANT (101). However, this process is reversible, meaning that, when mitochondrial respiration is not working properly, ANT has the opposite role, importing ATP produced via glycolysis into the mitochondria (101). Then, ATP can be hydrolyzed by the ATP-synthase working in reverse mode, which allows the maintenance of $\Delta\Psi m$ (102).

ANT is thought to influence cell death through pro-apoptotic proteins, such as Bax (103), or through mPTP (104). The exact role of ANT in the activity of mPTP is not completely understood, and there are some controversy studies regarding this subject. mPTP opening, which can be induced by Ca^{2+} and other factors, results in the dissipation of membrane potential and mitochondrial swelling, which ultimately leads to cell death (100). Several initial studies suggested that ANT is a key component of mPTP (105, 106) but, in contrast, later studies showed that although the ANT may have a regulatory role, it is not essential to its function (107).

There are four isoforms of ANT in humans: ANT1, ANT2, ANT3 and ANT4, and their expression is dependent on cell type, nature of the tissue, developmental stage and status of cell proliferation (Table 1) (108). ANT1, 3 and 4 are responsible for the mitochondrial export of ATP and import of ADP. ANT2 does the opposite, meaning that it imports ATP produced via glycolysis into the mitochondria and export ADP (108). Besides that, they are also involved in cell death pathways, performing opposite functions to regulate cell fate decisions, with some isoforms behaving like pro-apoptotic and others as anti-apoptotic

(109). ANT2 has also been associated with cancer and undifferentiated cells (108), and the current knowledge about its role in that is elucidated in the next section.

Table 1 - Human ANT isoforms are differentially expressed depending on tissue types, and they also have different functions as ATP/ADP exchangers.

Protein Isoform	ATP/ADP Exchange	Apoptosis Induction	Expression
ANT1	Export of ATP from the mitochondria to the cytosol and import of ADP	Pro-apoptotic	Non-dividing differentiated cells/tissues; skeletal muscle, heart, and brain
ANT2	Import of ATP from the cytosol to the mitochondria and export of ADP	Anti-apoptotic	Proliferative and regenerative undifferentiated cells/tissues; lymphocytes, kidney, liver, and some types of cancers
ANT3	Export ATP from the mitochondria to the cytosol and import of ADP	Pro-apoptotic	Ubiquitous
ANT4	Export ATP from the mitochondria to the cytosol and import of ADP	Anti-apoptotic	Testis and germ cells

1.3.1. Adenine nucleotide translocator 2 and its role in cancer

ANT2 is specifically expressed in undifferentiated cells and in tissues that are able to proliferate and regenerate (for example, kidney and liver) (108). The expression of ANT2 has been shown to be growth-dependent and is considered as a marker of cell proliferation. Because of that, ANT2 has been studied in cancer cells and cell lines, and it is thought to be is essential to the metabolic adaptation of cancer cells during tumoral development (55, 110). ANT2 was shown to be

overexpressed in various types of cancer (111), and is correlated with a higher glycolytic metabolism (110). Furthermore, some studies revealed that its silencing showed to increase apoptosis and decreased cell growth in human breast cancer cells (112) and breast cancer stem-like cells (113).

Since cancer cells rely mostly on the glycolytic pathway, ANT2 could be crucial as it is involved in the import of ATP generated via glycolysis to the mitochondria (108). Besides that, ANT2 is also known to prevent apoptosis and to contribute to the maintenance of the mitochondrial membrane potential (114). Most cancer cells present an increased mitochondrial membrane potential and ANT2 expression, being also able to resist cell death by apoptosis. However, through time there some loss of $\Delta\Psi m$ occurs. So, in order to avoid that, it is thought that cancer cells uptake ATP produced via glycolysis through ANT2, that will be used by ATP synthase working in reverse mode to avoid the decrease in membrane potential and allowing cell survival from induced apoptosis (55, 115).

It was also demonstrated that ANT protein levels were differently expressed in P19 embryonal carcinoma stem cells (Fig. 4) relative to their differentiated counterparts, showing an increased amount in P19dCs (86). These cells, first isolated by Rogers and McBurney (116) from a teratocarcinoma, are pluripotent and maintain a stem-like state in culture or can be differentiated to all three germ layers (endo, meso, and ectoderm) (117). Differentiation can be induced using non-toxic concentrations of Retinoic Acid (RA) (86). Given these unique characteristics, they are a good model to study CSCs and to compare to their differentiated counterparts by using only one cell line. In these cells, mRNA levels from ANT1 and ANT2 were shown to be overexpressed in P19dCs and in P19SCs, respectively. However, more studies regarding the protein levels of each ANT isoforms need to be done in order to better understand which isoform is responsible for that difference and what is its role in cancer stem cells metabolism. This could be important because, in the same study, it was also

demonstrated that P19SCs possess a higher glycolytic profile than their differentiated counterparts and their mitochondrial biology is also different. These results and the work done by Jang et al. (113) suggest that ANT2 may play a role in the metabolic remodeling of CSCs.

Thus, altogether, these findings support the idea that ANT2 could be crucial to the metabolic remodeling of CSCs and could be a possible target for future anti-cancer therapies.

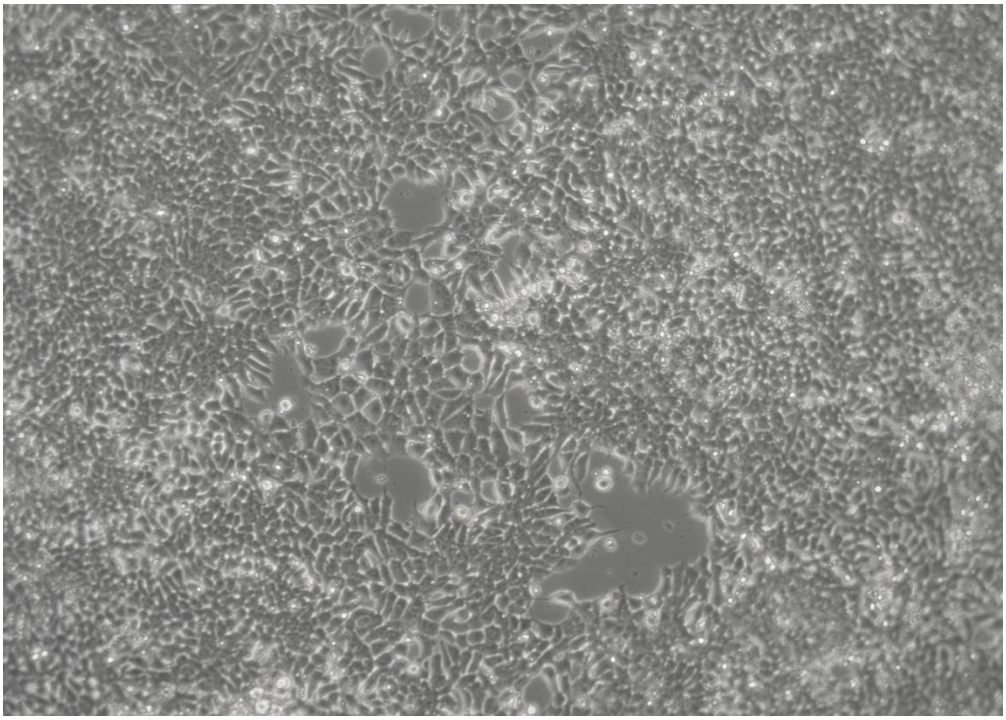

Figure 4 – Undifferentiated P19 cells. Image obtained using a 10x objective, Zeiss Primovert microscope with an Axiocam ERc 5s camera, using ZEN 2.3 software.

1.4. Objectives

Cancer cells have the ability to remodel their metabolism, which gives them several advantages, allowing them to adapt to different stresses, and to grow and proliferate without control. Moreover, cancer stem cells are described as having huge metabolism plasticity, being more glycolytic or more oxidative in a type-dependent manner, which probably can explain their capacity to resist to conventional anti-cancer therapies, as well being responsible for heterogeneity present within a tumor. Furthermore, several pieces of evidence showed that mitochondria play an important role in maintaining stemness properties (92). However, much is still unknown regarding this subject.

ANT2 is a mitochondrial protein largely involved in cancer metabolism. It was found that ANT isoform levels are different between CSCs and their differentiated counterparts (86) and ANT2 is known to be overexpressed in cancer cells (118). However, its role in mitochondrial metabolism is not completely understood.

Using P19 embryonal carcinoma stem cells as *in vitro* model, we hypothesized that ANT2 protein levels are increased in P19SCs when compared with P19dCs, and so, ANT2 could potential play an important role in the metabolic phenotype of CSCs. To uncover ANT2 underlying mechanisms in mitochondrial remodeling, our main goals are to 1) disclose whether ANT2 isoform is overexpressed in P19SCs, 2) evaluate if ANT2 silencing induces changes in P19SCs survival and growth, and 3) determine if P19SCs can remodel their metabolism by changing the ANT2 expression levels.

2. Material and Methods

2.1. Reagents

Table 2 - Reagents list.

Reagent	Company and Reference
40% Acrylamide/Bis Solution	Bio-Rad 1610148
Absolute Ethanol	Fisher E/0650DF/77
Ammonium Persulfate (APS)	Gerbu 1708-0020
Antibiotic-Antimycotic (100X)	Gibco 15240062
Antimycin A	Sigma-Aldrich A8674
ANT2 siRNA Oligonucleotide	Qiagen SI01421483
Bisbenzimide Hoechst 33342 Trihydrochloride	Invitrogen H1399
Blotting-Grade Blocker (nonfat dry milk)	Bio-Rad 1706404
Bovine Serum Albumin (BSA)	Sigma-Aldrich A6003
D-(+)-Glucose	Sigma-Aldrich G7021
Disodium Hydrogen Phosphate (Na_2HPO_4)	Sigma-Aldrich S5136
DMSO	Santa Cruz sc-359032
Dithiothreitol (DTT)	Sigma-Aldrich D9779
Dulbecco's Modified Eagle's Medium (DMEM)	Sigma-Aldrich D5030
Dulbecco's Modified Eagle's Medium (DMEM)	Sigma-Aldrich D5648
Ethanol	Panreac 121086.1212
FCCP	Santa Cruz sc-203578A
Fetal Bovine Serum (FBS)	Gibco 10270106
Glacial Acetic Acid	Panreac 131008.1611
Glycine	Fisher BP381-1
Hydrochloric Acid (HCl)	Panreac 131020.1212
L-Glutamine	Sigma-Aldrich G3126
Lipofectamine® 2000	Invitrogen 11668-019
Methanol	Fisher M/4056/17
N,N,N′,N′-Tetramethylethylenediamine (TEMED)	NzyTech MB03501

Negative Control siRNA Oligonucleotide	Qiagen 1027310
Oligomycin	Sigma-Aldrich O4876
Opti-MEM™ I Reduced Serum Medium	Thermo Scientific 31985070
Phenylmethanesulfonyl Fluoride (PMSF)	Sigma-Aldrich P7626
Pierce™ BCA Protein Assay Kit	Thermo Scientific 23227
Poly-D-lysine	Sigma-Aldrich P7280
Ponceau S	Sigma-Aldrich P3504
Potassium chloride (KCl)	Sigma-Aldrich P9541
Potassium Phosphate Monobasic (KH_2PO_4)	Sigma-Aldrich P0662
Protease Inhibitor Cocktail (PIC)	Sigma-Aldrich P8340
Resazurin Sodium Salt	Sigma-Aldrich R7017
Resolving Gel Buffer (1.5 M Tris-HCl)	Bio-Rad 161-0798
Rotenone	Sigma-Aldrich R8875
Seahorse XF Calibrant Solution	Agilent 100840-000
Sodium Bicarbonate ($NaHCO_3$)	Sigma-Aldrich S6014
Sodium Chloride (NaCl)	Sigma-Aldrich S7653
Sodium Deoxycholate	Sigma-Aldrich D6750
Sodium Dodecyl Sulphate (SDS)	Nzytech MB01501
Sodium Fluoride (NAF)	VWR
Sodium Hydroxide (NaOH)	Sigma-Aldrich S8045
Sodium Ortho Vanadate (Na_3VO_4)	Sigma-Aldrich S6508
Sodium Pyruvate	Sigma-Aldrich P2256
Stacking Gel Buffer (0.5 M Tris-HCl)	Bio-Rad 161-0799
Sulforhodamine B Sodium Salt	Sigma-Aldrich S9012
Tetramethylrhodamine (TMRM), Methyl Ester, Perchlorate	Thermo Scientific T668
Trans-Blot® Turbo™ 5x Transfer Buffer	Bio-Rad 10026938
Trichloroacetic Acid (TCA)	Sigma-Aldrich T0699
Tris Base	Nzytech MB01601
Triton X-100	Across Organics 327371000
Trypsin-EDTA (0.05%)	Gibco 25300062
Tween® 20	Fisher BP337-500

Table 3 - Solutions Preparation List.

Solution	Solution Preparation
Acetic acid solution in methanol, 1% (v/v)	For a total volume of 500mL, 5mL of 99,7% (v/v) glacial acetic acid was added in 495mL of 100% methanol. The solution was then stored at -20ºC.
Acetic acid solution, 1% (v/v)	For a total volume of 1L, 10 mL of 99,7% (v/v) glacial acetic acid was added to 990mL of MiliQ-purified water. The solution was stored at room temperature.
Growth Medium • ***1.8 g/l $NaHCO_3$*** • ***110 mg/l Sodium Pyruvate*** • ***10% FBS*** • ***1% antibiotic/antimycotic***	For a total volume of 500mL, 6.7g of DMEM5648, 0.9g NaHCO3, and 0.055g Sodium Pyruvate were added to 400mL of MiliQ-purified water. pH was adjusted to 7.2 and the volume was then adjusted to 445mL. In the flow chamber, the medium was filtered using filtration units (514-0332, VWR), and 5mL of antibiotic/antimycotic solution and 50mL pf FBS were added. The solution was stored at 4ºC.
MitoStress Medium • ***25mM Glucose*** • ***1mM Sodium Pyruvate*** • ***4mM L-Glutamine***	For a total volume of 70mL, 1.4mL of 1.25M Glucose, 700uL 100mM Sodium Pyruvate, and 1.4mL of 200mM L-Glutamine were added to DMEM5030. pH was adjusted to 7.4 with 0.1M NaOH.
Phosphate-buffered saline 10X • ***137mM NaCl*** • ***2.7mM KCl*** • ***4.3mM Na_2HPO_4*** • ***1.5mM KH_2PO_4***	For a total volume of 1L, 80f of NaCl, 2g of KCL, 6.09g of Na_2HPO_4 and 2g of KH_2PO_4 were dissolved in MiliQ-purified water. pH was adjusted to 7.2. To prepare **PBS 1X**, 100mL of PBS 10X were diluted in 900mL of MiliQ-purified water. The solution was stored at room temperature.
Ponceau S solution • ***0.1% (w/v) in 5% Acetic acid***	For a total volume of 100 mL, 0.5g of Ponceau S were diluted in 95mL of MiliQ-purified water and 5mL of 99,7% (v/v) glacial acetic acid. Solution stored at 4ºC, protected from light.
Resazurin solution	10 mg of resazurin sodium salt was dissolved in 10 mL of PBS and filtered with 0.2 μm pore filter. Stored at -20 ºC.

RIPA buffer • ***150mM NaCl*** • ***1% Triton X-100*** • ***0.5% Sodium Deoxycholate*** • ***0.1% SDS*** • ***50 mM Tris pH 8***	For a total volume of 10mL, 1.5mL of 1M NaCl, 100µL of Triton X-100, 500µL of 10% SDS and 1mL of 500 mM Tris pH 8 were mixed and MiliQ-purified water was added till the desired volume.
Running Buffer 10X • ***25 mM Tris*** • ***192 mM glycine*** • ***0.1% SDS***	For a total volume of 1L, 150g of Glycine, 30g of Tris, and 10g of SDS were dissolved in MiliQ-purified water. Solution stored at room temperature. To prepare **running buffer 1X**, 100mL of running buffer 10X were diluted in 900mL of in MiliQ-purified water, and the solution was stored at 4ºC.
Sulforhodamine B (SRB) solution	The SRB solution was prepared with 0.25 g of SRB dissolved in 500 mL of 1% (v/v) acetic acid in MilliQ-purified water. The solution was stored at 4 °C, protected from light.
TBS 10X • ***1.5M NaCl*** • ***100 mM Tris base***	For a total volume of 1 L, 87.12g of NaCl and 12.2g of Tris were dissolved in MilliQ-purified water. Stored at room temperature.
TBS-T (1X) (Washing Buffer) • ***150 mM NaCl*** • ***10 mM Tris base*** • ***0.1% Tween® 20***	For a total volume of 1 L, 100 mL of TBS 10X and 1mL Tween 20 were diluted in 900mL of MilliQ-purified water. Stored at room temperature.
Transfer Buffer	For a total volume of 250mL, 150ml of MilliQ-purified water, 50mL of ethanol and 50mL of Trans-Blot® Turbo™ 5x Transfer Buffer were mixed.
Tris-NaOH 10.5 mM	0.64g of Tris was dissolved in 400mL of MiliQ-purified water by agitation. pH was adjusted to 10.5 with 1M of NaOH. Volume was adjusted to 500mL with MiliQ-purified water. Store at room temperature.

2.2. Methods

2.2.1. Cell culture

The P19 embryonal carcinoma cell line (P19SCs) used in this work was obtained from the American Type Culture Collection (ATCC® CRL-1825™) (Fig. 4) and cultured in High glucose Dulbecco's modified Eagle's medium (DMEM-D5648) at 37ºC in a humidified atmosphere of 5% CO_2, in 100 mm-diameter tissue culture dishes. The medium was supplemented with 10% FBS, 1.8 g/l sodium bicarbonate, 110 mg/l sodium pyruvate, and 1% antibiotic/antimycotic solution. Cells were passaged every 2-3 days when reaching 70-80% confluence. In each passage, the medium was removed, and the plates were washed with 1× Phosphate Buffered saline (PBS). Then, the cells were incubated with 0.05% trypsin/EDTA at 37ºC and in a 5% CO_2 atmosphere for at least 3 minutes. Trypsin activity was inactivated by adding the same volume of fresh medium, and the cell suspension was centrifuged at 250xg for 5 minutes. After that, a 1:20 to 1:30 dilution was performed in a new 100 mm plate and cells were incubated in a humid atmosphere with 5% CO_2 at 37ºC.

For cell counting, 10 µl of each cellular suspension was diluted in 0.4% (w/v) Trypan blue solution in a ratio of 1:1, and the suspension was imaged in Bio-Rad® TC20™ Automated Cell Counter (Bio-Rad Laboratories).

2.2.2. Cell differentiation

To induce cell differentiation, P19 cells were seeded at a density of $5{,}2x10^3$ cells/cm^2 and 1 µM of Retinoic Acid was added for 96h. After that time, P19 stem cells (P19SCs) and P19 differentiated cells (P19dCs) were collected to perform the necessary experiments.

2.2.3. Cell morphology

For morphological studies, images were taken using a Zeiss Primovert microscope with an Axiocam ERc 5s camera, using ZEN 2.3 software, with 10X and 20X objectives.

2.2.4. Cell transfection and ANT2 silencing using siRNA

Transfection is a process of introducing foreign nucleic acids into cells in order to produce genetically modified cells. Small-interfering RNA (siRNA) is commonly used in transfection experiments, allowing to study the short-term impact of alterations in gene and protein expression. siRNA is a class of double-stranded RNA molecules with 20-25 base pairs, that prevents translation by degrading mRNA. siRNAs interfere with the expression of specific genes with complementary nucleotide sequences (119).

To facilitate siRNA delivery into cells, Lipofectamine® 2000 was used. Lipofectamine is a cationic lipid-based chemical transfectant and, because it has a positive charge, it forms liposomes when in contact with nucleic acids (negatively charged). Then, these transfection complexes (lipofectamine including siRNA) fuse with the cell membrane and release their cargo inside the cell (119).

P19SCs were transfected with 50 nM of ANT2 siRNA oligonucleotide (siANT2), sense strand 5'- CGA GCU GCC UAC UUU GCU ATT – 3', antisense strand 5'- UAC CAA AGU AGG CAG CUC GGT - 3', or with a scrambled siRNA as a negative control (siControl), SENSE STRAND 5' – UUC UCC GAA CGU GUC ACG UdT dT – 3', antisense strand 5'- ACG UGA CAC GUU CGG AGA AdT dT -3', that were prepared following the manufacturer's instructions in order to obtain a 20μM stock solution. To perform the assay, cells were seeded at a density of $7.5x10^3$ cell/cm^2, in a 6 multi-well plate. After 24 hours of incubation,

transfection was done using Lipofectamine 2000 transfection reagent and two sets of Eppendorf's were prepared: the first one (A and B) with oligonucleotides, and the second (A' and B') with Lipofectamine (Fig.5). In order to obtain a final concentration of 50 nM, 2.5µL of negative control or ANT2 oligonucleotides were diluted in OptiMEM at room temperature for 5 minutes, in a final volume of 125µL. In the other set of tubes, 5 µL of Lipofectamine 2000 were incubated in OptiMEM, also in a final volume of 125µL per tube. After that, the content of tube A and B was mixed with A' and B', respectively, and incubated at room temperature for 20 minutes. The complexes were then added to each well, containing 750µL of serum and antibiotic-free medium, by gently pipetting 250µL of transfection agent, dropwise, in a final volume of 1mL (Fig.4). Following 5 hours of incubation at 37ºC and 5% CO_2 atmosphere, transfection media was

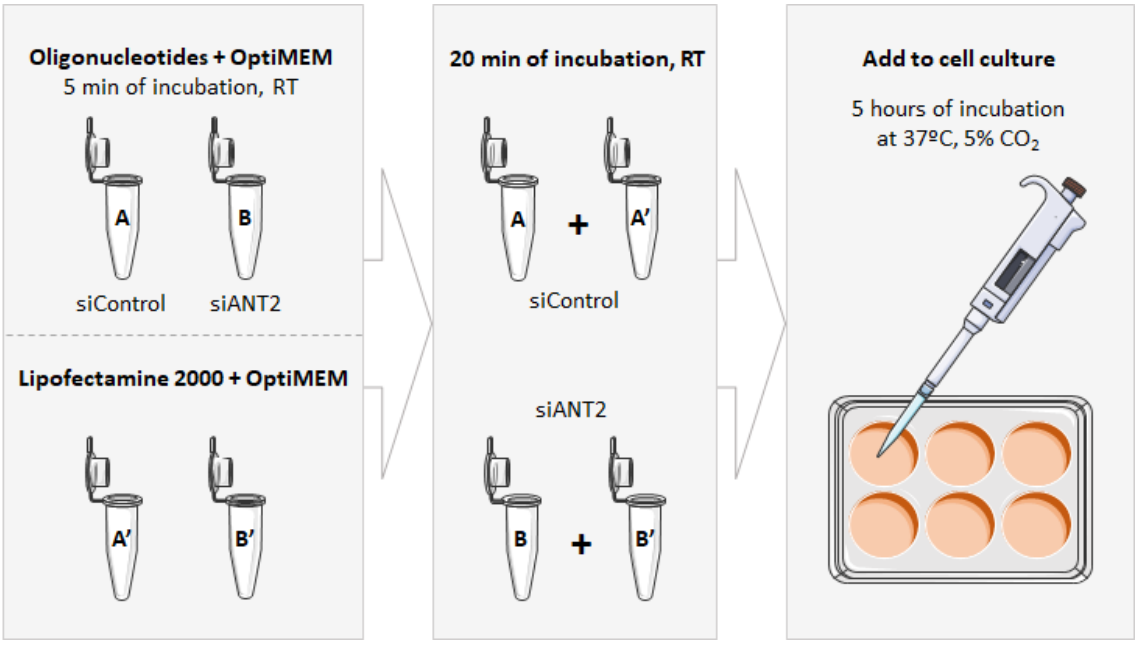

Figure 5 - Cell transfection using siRNA for ANT2 silencing. Two sets of Eppendorf's were labeled (A and B; A' and B'B). In the first set of tubes (A and B), OptiMEM and 50nM of ANT2 or negative control siRNA were added. Then, in tubes A' and B', Lipofectamine was added to OptiMEM. After 5 minutes of incubation at room temperature, the content of Eppendorf A was added to Eppendorf A', and B to B'. After 20 minutes of incubation, at room temperature, 250µL of the complexes mixture was carefully and dropwise added to each well. Cells were incubated a 37ºC for 5 hours, after which the content of each well was aspirated, and 3 mL of fresh complete growth medium was added.

replaced by 3 mL of complete growth medium and the plate with the cells placed again in the incubator.

For resazurin and SRB assays (Section 2.2.7 and 2.2.8), cells were plated in a 96 multi-well plate and the conditions of transfection were maintained and adapted to the area and volume of the plate.

2.2.5. Protein extraction and quantification

In order to evaluate protein levels in different conditions, Western blotting was performed. Cells were harvest after trypsinization, centrifuged for 5 minutes, then washed with PBS 1X and centrifuged again. The cell pellet was resuspended in RIPA buffer supplemented with 2mM DTT, 100 mM PMSF, 20mM NAF, 80mM Na_3VO_4 and a protease inhibitor cocktail (1:100). n samples were then sonicated and kept at -80ºC until further use.

Pierce™ Bicinchoninic Acid (BCA) Protein Assay Kit was used to determine the protein content of each sample, and Bovine Serum Albumin (BSA) solutions were used as standards. Diluted samples and standard solutions were added to a 96 multi-well plate and 200µL of working reagent was added to each well. The plate was incubated in the dark at 37ºC, and then the absorbance was measured using BioTek® Cytation3™ UV–vis multi-well plate imaging reader.

2.2.6. Western blotting

After protein quantification, samples were denatured with Laemelli buffer - DTT at 95°C for 5 minutes (except for OXPHOS complexes protein levels). Then, 20 µg of protein were loaded in a 12% sodium dodecyl sulfate (SDS)-polyacrylamide gel (SDS-PAGE) and separated by electrophoresis at 120V, for 90 minutes, at room temperature using PowerPac™ Basic Power Supply (Bio-Rad

Laboratories). Then, the protein was transferred from the gel to a polyvinylidene difluoride (Bio-Rad, 1704273) or nitrocellulose (Bio-Rad, 1704271) membrane at 25V, for 10 min, using the Trans-Blot® Turbo™ Transfer System (Bio-Rad Laboratories). Membranes were stained with Ponceaus S solution to ensure that protein was transferred and normalization purposes in specific cases. After Ponceau destaining and blocking step with 5% non-fat dry milk in TBS-T at room temperature, for 2 hours, membranes were incubated with primary antibody (Table 4) at 4ºC, overnight, under continuous stirring. After three washes with

Table 4 - Antibodies used in Western blotting analysis.

Antibody	MW (kDa)	Host Species	Dilution	Reference and Company
ANT 1/2	33	Goat	1:500 in 5% milk in TBS-T	sc-9299 Santa Cruz
ANT2	29	Rabbit	1:500 in 5% milk in TBS-T	14671 Cell Signaling
β-Actin	43	Mouse	1:5000 in TBS-T	MAB1501 Millipore
βIII-Tubulin	55	Mouse	1:500 in TBS-T	sc-80005 Santa Cruz
Drp1	80	Mouse	1:200 in 5% milk in TBS-T	sc271583 Santa Cruz
HKII	102	Rabbit	1:500 in 5% BSA in TBS-T	286, Cell Signaling
Mfn1	86	Rabbit	1:250 in 5% milk in TBS-T	sc-50330 Santa Cruz
OCT4	45	Rabbit	1:500 in 5% milk in TBS-T	2840 Cell Signaling
Total OXPHOS Rodent Antibody Cocktail	20, 30, 40, 48, 55	Mouse	1:1000 in 5% milk in TBS-T	ab110413 abcam
PDK	49, 46, 47	Rabbit	1:500 in 5% BSA in TBS-T	sc-28783 Santa Cruz
PGC1-a	90	Rabbit	1:500 in 5% milk in TBS-T	sc-13067 Santa Cruz
PKM2	60	Rabbit	1:500 in 5% BSA in TBS-T	4053 Cell Signaling
TFAM	25	Goat	1:750 in 5% milk in TBS-T	sc-23588 Santa Cruz
TOM20	20	Rabbit	1:1000 in TBS-T	sc-11415 Santa Cruz
TROMA-I	55	Mouse	1:500 in 5% milk in TBS-T	DSHB
Anti-Goat	-	Mouse	1:2500 in TBS-T	sc-2354 Santa Cruz
Anti-Mouse	-	Horse	1:2500 in TBS-T	7076 Cell Signaling
Anti-Rabbit	-	Goat	1:2500 in TBS-T	7074 Cell Signaling

TBS-T, 5 minutes each, membranes were incubated with the respective Horseradish Peroxidase (HRP)-conjugated secondary antibody (Table 4) for 1 hour at room temperature. Afterward, membranes were washed again with TBS-T and incubated with Clarity™ Western ECL Substrate detection kit (Bio-Rad, 1705061). Image acquisition was performed using VWR Gel Documentation System Imager Chemi 5QE. Band densities were quantified using TotalLab TL120 software.

2.2.7. Resazurin assay

Resazurin assay allows measuring metabolic activity as an indicator of cell viability. This assay is based on the reduction of resazurin to resorufin, a pink fluorescent dye, through dehydrogenases activity in viable cells with active metabolism (120, 121).

P19SCs were plated on 96 multi-well plates with a cellular density of $7.5x10^3$ cell/cm^2 and, 24 hours later, they were transfected with Control and ANT2 siRNA (accordingly to Section 2.2.3). After 24, 48, 72 and 96 hours of transfection, the medium was completely removed and fresh medium with 10 μg/ml of resazurin was added to the cells. Plates were then incubated in the dark at 37°C and with a 5% CO_2 atmosphere, for 90 minutes (48, 72 and 96 hours of transfection) or 4 hours (24h of transfection). The amount of resazurin reduced to resorufin was then measured through fluorescence measurements at an excitation wavelength of 540nm and emission wavelength of 590nm, using BioTek® Cytation3™ UV–vis multi-well plate imaging reader (BioTek) (121).

After the assay, the medium was completely removed, wells were washed with PBS 1X and then fixed with 100μL of ice-cold 1% (v/v) acetic acid in methanol. The plates were kept at -20ºC, at least overnight, to then perform SRB assay, allowing to have distinct experiments in the same plates.

2.2.8. Sulforhodamine B assay

Sulforhodamine B (SRB) assay is a colorimetric assay, and the principle behind it is based on the ability of SRB, a pink dye, to bind to protein basic amino acid residues (122, 123). Thus, this assay provides an estimation of cellular protein content which, in turn, is directly related to cell mass.

After having the cells fixed with ice-cold 1% (v/v) acetic acid in methanol, as explained in the previous section, and to perform the SRB protocol, the content of each well was discarded, and the plates were left to dry at 37ºC. Then, the SRB solution (0,5% in 1% acetic acid) was added to each well and incubated at 37°C for 1 hour. Afterward, SRB was discarded and the wells were washed with 1% (v/v) acetic acid in order to remove SRB excess. Plates were dried at 37ºC and the SRB dye was resuspend with a solution of 10 mM Tris pH 10. Absorbance was measured at 510nm and background measurement at 620nm, using BioTek® Cytation3™ UV–vis multi-well plate imaging reader.

SRB assay was also used for normalization purposes of Seahorse assay (Section 2.2.8). In this case, after the MitoStress protocol, cells were fixed using 50µL of 60% (w/v) trichloroacetic acid (TCA) (final percentage of 10%) in each well, being incubated overnight at 4°C. After that time, the content of each well was removed and discarded, the plate was washed with distilled water and dried at 37ºC. The subsequent protocol was the same as described in the previous paragraph.

2.2.9. Cellular oxygen consumption measurements

Oxygen consumption rate (OCR) and extracellular acidification rate (ECAR) were measured using a Seahorse XFe96 Extracellular Flux Analyzer (Agilent) by performing XF Cell MitoStress Seahorse assay. In this assay, different modulators are used to target specific components of ETC, allowing to

calculate different parameters regarding mitochondrial function. Oligomycin is used to inhibit ATP synthase (Fo subunit of complex V), FCCP is an uncoupler that induces the dissipation of the electrochemical proton gradient, and Antimycin and Rotenone inhibit complex III and complex I, respectively (Fig. 6).

In the day before the assay, XFe96 sensor cartridge was left to hydrate with 200 µl per well of sterile water overnight at 37°C in a non-CO_2 incubator. An aliquot of Seahorse XF Calibrant was also left overnight in the same conditions as the cartridges.

In order to prevent cell detachment during the assay, each well of Agilent Seahorse XF96 Cell Culture Microplates (101085-004, Agilent) was coated with 30µL of poly-D-lysine for, at least, 1 hour at 37ºC. Then, poly-D-lysine was removed, and the wells were washed with sterile water. The plate was left to dry in the flow chamber for 1 hour.

On the previous day to the MitoStress assay, transfected P19SCs cells (24h) were plated in order to evaluate the silencing effect after 48 hours of transfection. Cells were seeded at a cellular density of 35.000 cells/well in 80µl of culture

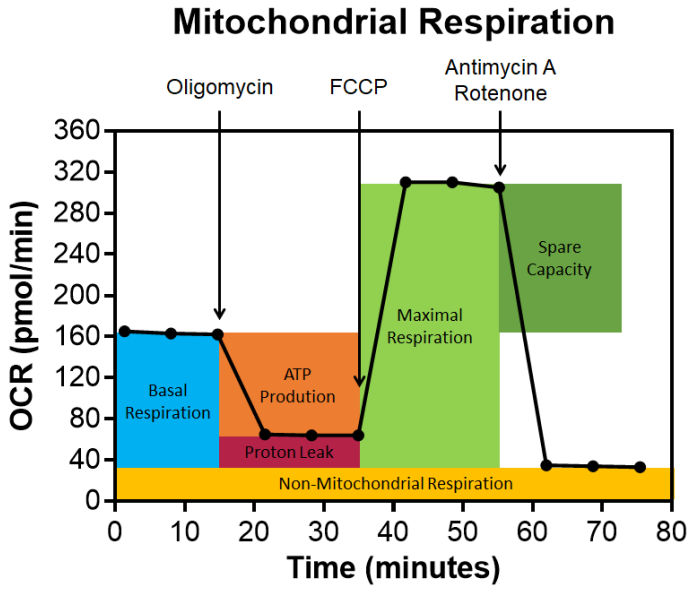

Figure 6 - Seahorse XF Cell MitoStress assay profile and associated parameters.

medium on the Agilent Seahorse XF96 Cell Culture Microplates coated with poly-D-lysine.

In the day of the assay, the sterile water in the calibration plate containing the XFe96 sensor cartridge was discarded and 200µL of Seahorse XF Calibrant was added to each well for 45-60 minutes at 37ºC. One hour before the assay, microplates containing cells were washed three times with MitoStress medium, pre-heated at 37ºC. In the last wash, 175µL of medium was left in the wells and the plate was incubated at 37ºC for 1h.

Stock solutions of Oligomycin, FCCP, Antimycin A and Rotenone (2,5mM each) were prepared previously in DMSO. Before the assay, the drug solutions that were loaded on the injection ports were prepared in MitoStress medium. Concentrated solutions of these drugs were prepared to obtain 3µM of oligomycin, 0.25µM of FCCP and 1µM of Rotenone + Antimycin A, as final concentrations. Then, 25µL of each solution was loaded to the corresponding injection port on sensor cartridge: Oligomycin – Port A; FCCP – Port B; Rotenone + Antimycin A – Port C.

The calibration plate was placed with the XFe96 loaded sensor cartridge on the instrument tray to calibrate and, next, the calibration plate was replaced by the cell culture microplate to the MitoStress assay takes place. Drugs were then injected automatically into each well, port by port.

All data were normalized by cell mass, measured by SRB assay, as described in Section 2.2.8. After normalization, data analysis was done with the Seahorse MitoStress Test Report Generator, using the Software Version Wave Desktop 2.2 from Agilent, that automatically calculates different parameters regarding mitochondrial function (Table 5). The generator allows calculating Basal Respiration, ATP Production, Proton Leak, Maximal Respiration, Spare Respiratory Capacity, Non-Mitochondrial Respiration, and Extracellular Acidification Rate.

Table 5 - Mitochondrial parameters and equations to calculate them.

Parameter	Formula
Basal Respiration	(Late rate measurement before 1st injection) – (Non-mitochondrial respiration rate)
ATP Production	(Late rate measurement before oligomycin injection) – (Minimum rate measurement after oligomycin injection)
Proton Leak	(Minimum rate measurement after oligomycin injection) – (Non-mitochondrial respiration)
Maximal Respiration	(Maximum rate measurement after FCCP injection) – (Non-mitochondrial respiration)
Spare Respiratory Capacity	(Maximal respiration) – (Basal Respiration)
Non-Mitochondrial Respiration	Minimum rate measurement after Rotenone and Antimycin A injection

2.2.10. Fluorescence microscopy imaging

Mitochondrial membrane potential (ΔΨm) and Mitochondrial network measurements were done by labeling mitochondria with Tetramethylrhodamine methyl ester (TMRM). TMRM is a red-fluorescent cell-permeant dye that accumulates in active mitochondria with intact membrane potential (negatively charge polarized mitochondria).

Transfected cells were seeded in μ-Slide 8 Well ibiTreat (80826, Ibidi) at a cellular density of 30.000 cells per well (24 hours after transfection). Then, 24 hours after seeding, the medium was completely removed and cells were incubated with 100 nM TMRM and 1 μg/ml Hoechst 33342, prepared in fresh complete growth medium, for 30 minutes, in the dark, at 37°C and with a 5% CO_2 atmosphere. All images were collected at 63X magnification (numerical aperture: 1.4), in Carl Zeiss LSM 710 laser scanning confocal microscope, pre-heated at 37ºC, using Diode 405-30 (405nm) and DPSS 561-10 (561nm) lasers. Data were analyzed by selecting individual cells and also the hole cluster.

Image processing and analysis were performed using ImageJ 1.51u software. Mitochondrial network area was measured by two different approaches: 1) a threshold was applied to the images in order to select the area occupied by TMRM, and 2) TMRM area, calculated as explained previously, was divided by the total area of cell or cluster, in order to calculate the percentage of cells/cluster that was occupied by TMRM. For clusters of cells, the area was normalized by the number of nuclei present in each cluster. Mitochondrial membrane potential was assessed by measuring standard deviation and mean gray value of each cell or cluster of cells.

2.2.11. Statistical Analysis

All statistical analysis was performed using GraphPad Prism 8.0.2 software. Data were checked for normal distributions and homogeneity of variances by the Shapiro-Wilk test and the F-test, respectively. Student's t test was used for statistical analysis of two means. In cases were normality was not verified, the Mann-Whitney test was performed. Two-way ANOVA with Sidak's multiple comparisons was performed for statistical analysis of growth curves.

Results are presented as means ± SEM for the number of experiments indicated in the respective figure legend. Values with $p < 0.05$ were considered statistically significant.

3. Results

3.1. P19 cells differentiation and ANT levels

Vega-Naredo et al. showed that total protein levels of ANT1/2 were differently expressed in P19SCs when compared to their differentiated counterparts. However, the isoform responsible for that difference was not clarified. Therefore, the starting point of this project was to induce differentiation using retinoic acid and verify if ANT2 isoform is overexpressed in P19SCs.

P19SCs were treated with 1μM of retinoic acid for 96 hours and were visualized at the microscope in order to check for possible morphological differences. As shown in Figure 8.A, P19SCs were smaller than P19dCs and exhibited a more rounded shape, whereas P19dCs were more stretched, resembling neuronal cells.

Regarding differentiation markers, β-3-Tubulin and trophectodermal cytokeratin 8 Endo-A (TROMA-I) were increased in P19dCs comparatively to P19SCs (Fig. 8B-D). At the same time, the octamer-binding transcription factor (OCT4), which is a pluripotency marker, was decreased in P19dCs (Fig. 8E).

ANT1/2 levels were increased in P19dCs, confirming what was described by Vega-Naredo et al. (86). Then, ANT2 expression was also measured using a specific antibody for this isoform what allowed to observe a high protein content in P19SCs (Fig. 8B, 8F).

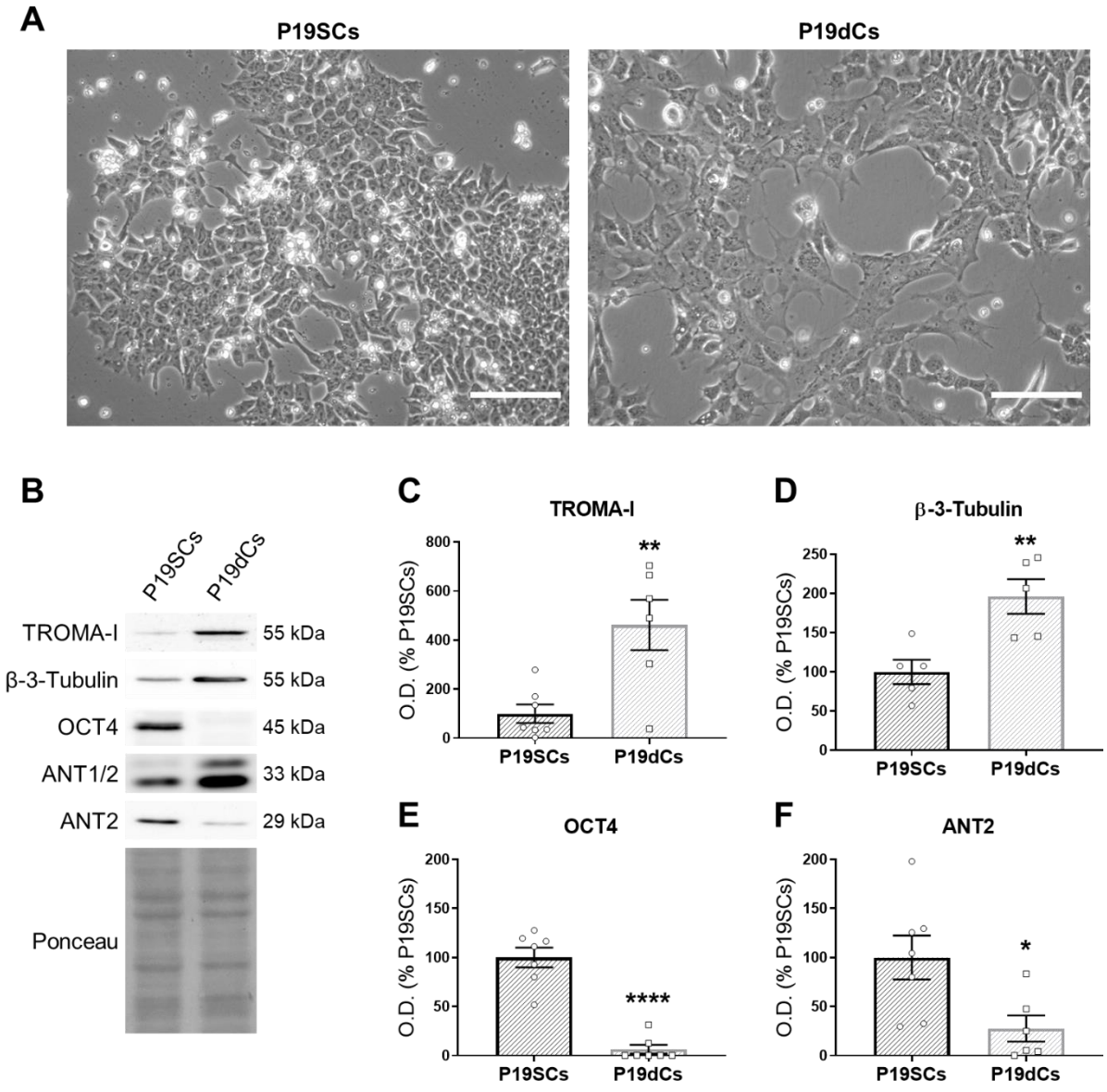

Figure 7 - Morphological changes and differential ANT isoforms expression in P19 cells. (A) Microscopy images of P19 embryonal carcinoma stem cells (P19SCs) and their differentiated counterparts (P19dCs) upon 1 μM retinoic acid treatment for 96h; 20X magnification and scale bar = 200μm. **(B)** Representative Western blotting of differentiation (TROMA-I and β-3-Tubulin) and pluripotency (OCT4) markers, and ANT1/2 and ANT2 proteins. Ponceau S was used for loading control and normalization purposes. **(C)(D)** TROMA-I, β-3-Tubulin and **(E)** OCT4 protein levels in P19SCs and P10dCs. **(F)** ANT2 isoform expression levels in P19SCs and P19dCs. Data are presented as mean ± SEM expressed as percentage of P19SCs from, at least, 5 independent experiments. Statistical analysis was performed using Student's t-test. *: $p<0.05$, **: $p<0.01$ and ****: $p<0.0001$.

3.2. Characterization of P19 ANT2 silenced cells

As ANT2 is known to be correlated with a glycolytic phenotype and, as we showed in the previous section, is increased in P19CSs, the next approach was to silence ANT2 by transfection, using siRNA, in order to study its role in the metabolic profile of the cells.

SiRNA transfection is transient, meaning that the nucleic acids introduced into the transfected cells are not permanently incorporated into the cellular genome, existing for a limited period of time (119). Thus, in order to choose the best timepoints and to confirm that silencing occurred, cells were collected at different times of transfection (24 – 120 hours). Then, ANT2 protein content was measured by Western blotting and, as it is possible to observe in Figure 8, it is clear that silencing occurred with a high rate of efficiency, with P19SCs transfected with ANT2 siRNA (siANT2) expressing highly decreased protein levels of ANT2 when compared with cells transfected with control siRNA (siControl), in all the time points (Fig. 8A-C). Accordingly to these results, the time points chosen for most of the subsequent protocols were 48 and 96 hours due to high efficiency and protein levels downregulation (Fig. 8A and B, respectively).

In order to verify if P19 cells maintain their stemness properties with ANT2 silencing, protein levels of pluripotency and differentiation markers were evaluated, as well as cell morphology. To do so, transfected cells were compared with P19SCs and P19dCs. TROMA-I and OCT4 protein levels were not affected by ANT2 silencing (Fig. 8D). Regarding cell morphology, transfected cells seemed similar to P19SCs (Fig. 8E), which suggest that ANT2 absence does not promote loss of stemness.

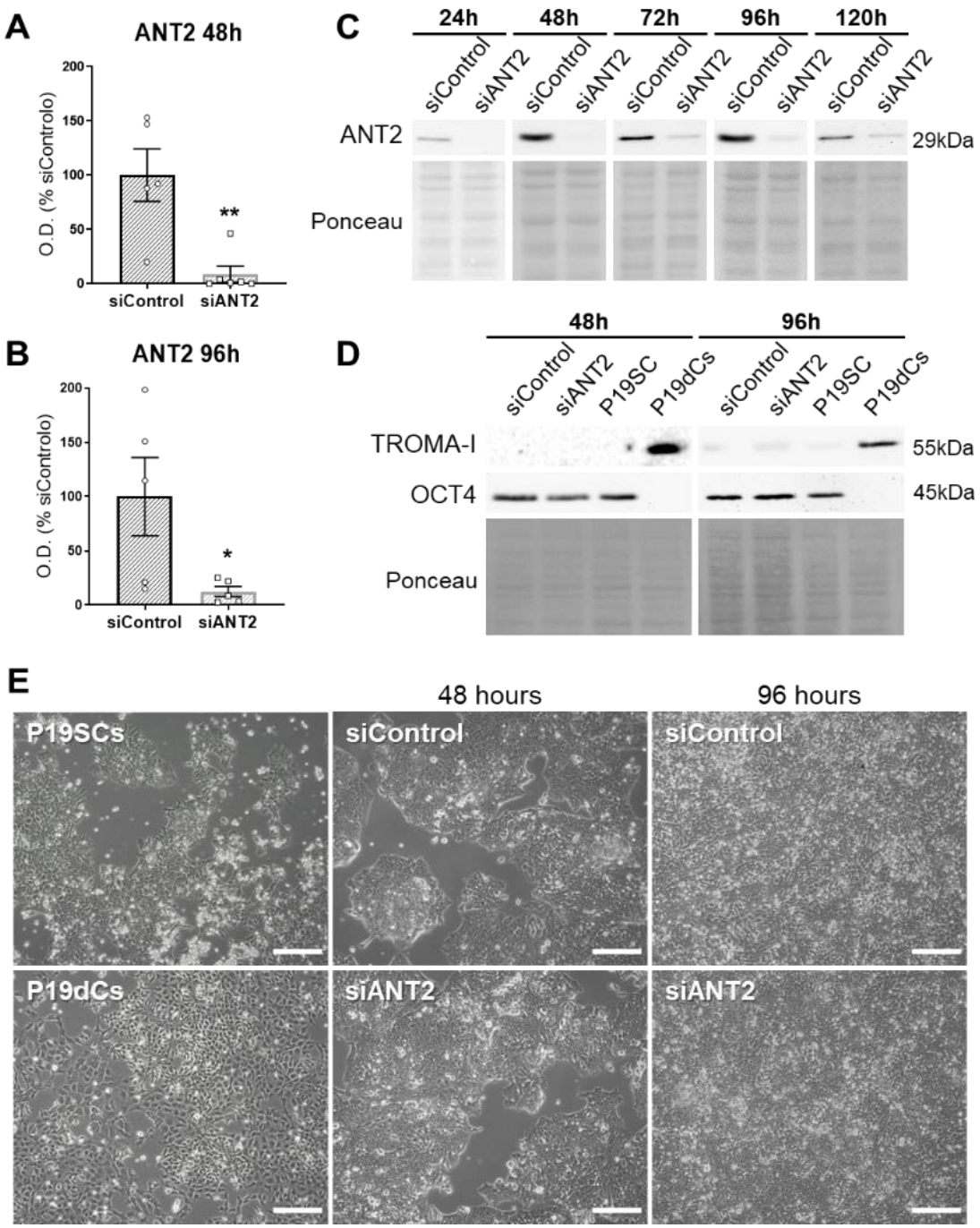

Figure 8 - Gene silencing decreased ANT2 protein expression levels through time, and did not promote differentiation of P19 cells. (A) Expression levels of ANT2 after 48 hours and **(B)** 96 hours after silencing. Data are presented as mean ± SEM expressed as percentage of siControl from, at least, 5 independent experiments. Statistical analysis was performed using Student's t-test. *: $p<0.05$, **: $p<0.01$ **(C)** Representative Western blotting of ANT2 after 24, 48, 72, 96 and 120 hours after transfection. Ponceau S was used for loading control and normalization purposes. **(D)** Representative Western blotting of TROMA-I (differentiation marker) and OCT4 (pluripotency marker) after 48 hours and 96 hours after silencing. Ponceau S was used for a loading control. **(E)** Microscopy images of P19 embryonal carcinoma stem cells (P19SCs), and their differentiated counterparts (P19dCs), and siControl and siANT2 cells after 48 and 96 hours of transfection with 10X magnification using Zeiss Primovert microscope. Scale bar = 200μm.

3.3. ANT2 silencing promoted a decrease in metabolic activity and cell mass in P19 cells

It was described by Jang et al. (113, 124) that ANT2 silencing in breast cancer and breast cancer stem-like cells promotes apoptosis and a diminish in tumor growth. Thus, we sought to investigate if P19 ANT2 silenced cells also have a decrease in cell growth when compared to siControl cells. In order to verify that, resazurin and SRB assays were performed to measure metabolic activity and cell mass, respectively. To do so, P19SCS were directly transfected in 96 multi-well plates. Silencing efficiency, under these conditions, was confirmed at 96 hours post-transfection by Western blotting analysis (Fig. 9A). Resazurin assay was done at 24, 48, 72 and 96 hours after transfection, followed by SRB assay. Metabolic activity decreased when comparing ANT2 silenced cells with the respective control at the same time point (Fig. 9B). In particular, at 48 and 72 hours after transfection, the decreased reached more than 20%, being also statistically significant ($p < 0.01$). The same happened with cell mass (Fig. 9C), especially at 48 hours, with a decreased of 35% and statistical significance ($p < 0.05$). Data analysis as percentage of 24 hours-siControl transfected cells was also made in order to better verify the effect of ANT2 silencing over time. Again, a lower metabolic activity rate (Fig. 9D) and cell mass (Fig. 9E) was observed in the ANT2 siRNA cells comparatively to the siControl group. Nevertheless, cells of both groups reached maximal confluence in the wells at 96 hours, as it is visible in Figure 9E. Since, a lot of dead cells were visible in suspension, indicative of possible cell death, we also saw a decrease in the metabolic activity (Fig. 9D).

These results suggest that ANT2 silencing induces a decrease in metabolic activity and cell mass in P19SCs.

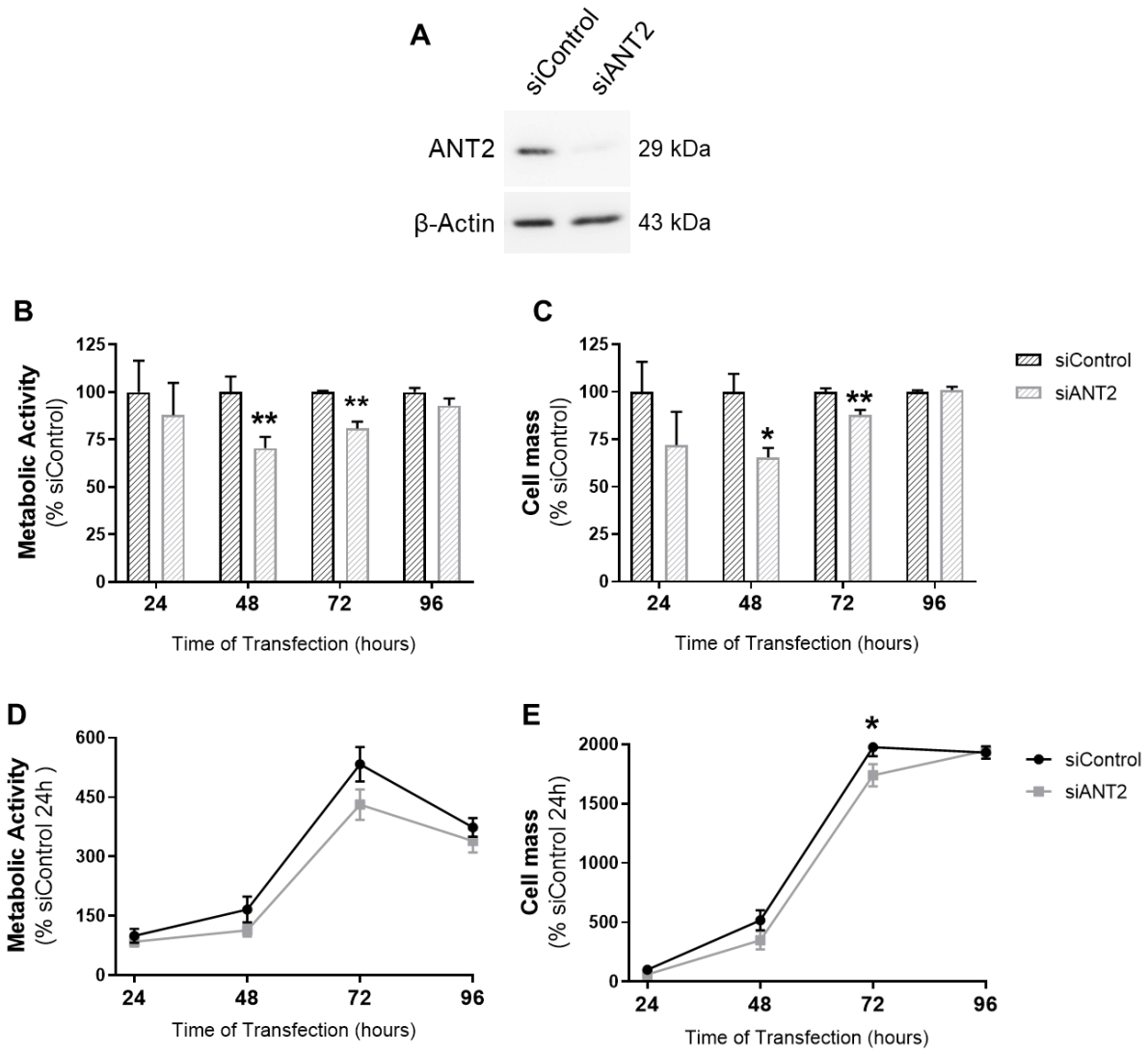

Figure 9 - Effect of ANT2 silencing on metabolic activity and cell mass in P19SCs. (A) Representative Western blotting of ANT2 protein levels in P19SCs after being transfected in a 96 multi-well plate. β-Actin was used as a loading control. **(B)** Metabolic activity measured by resazurin assay and **(C)** Cell mass measured by SRB after 24, 48, 72 and 96 hours after transfection. Data are presented as mean ± SEM expressed as percentage of the respective siControl from 5 independent experiments. Statistical analysis was performed using Student's t test for each time point. *: $p<0.05$, **: $p<0.01$ Metabolic activity measured by resazurin assay and **(C)** Cell mass measured by SRB after 24, 48, 72 and 96 hours after transfection. Data are presented as mean ± SEM expressed as percentage of siControl at 24h of transfection from 5 independent experiments. Statistical analysis was performed using two-way ANOVA test with Sidak's multiple comparisons. *: $p<0.05$

3.4. Effect of ANT2 silencing in cellular oxygen consumption measurements and OXPHOS complexes

Given the observed changes in the metabolic activity and cell mass following ANT2 silencing and the described link of ANT2 in cancer metabolic features and

role in the mitochondria, we thought to evaluate the potential effect of ANT2 downregulation at the mitochondrial level. Thus, mitochondrial respiration was analyzed by XF^{e}96 Cell MitoStress Seahorse^{TM} assay, and protein levels of OXPHOS complexes by Western blotting. The time points chosen were 48 hours of transfection for MitoStress protocol, and 48 and 96 hours for Western blotting. The choice was based on metabolic activity, where it was possible to observe a decrease of 30% for siANT2 cells with 48 hours of silencing. 96 hours were chosen in order to better understand the metabolic modifications that occur upon ANT2 downregulation along the time in P19 cells.

P19 transfected cells were subjected to MitoStress assay after 48 hours of silencing. Data of oxygen consumption rate (OCR) parameters, basal extracellular rate (ECAR), and OCR over time are represented in Figure 10.

Basal respiration, proton leak-dependent respiration, maximal respiration, and ATP production-linked respiration were significantly decreased in siANT2 cells (Fig. 10A-D). Regarding non-mitochondrial oxygen consumption, spare respiratory capacity, and basal ECAR, no significant differences were found (Fig. 10E-G). Based on the above data, the expression of subunits of the mitochondrial electron transport chain was evaluated in order to verify if OXPHOS machinery was remodeled. NADH dehydrogenase [ubiquinone] 1 β subcomplex subunit 8 (NDUFB8) from Complex I, Succinate dehydrogenase [ubiquinone] iron-sulfur subunit (SDHB) from Complex II, Cytochrome b-c1 complex subunit 2 (UQCRC2) from Complex III, cytochrome c oxidase subunit I (MTCO1) from complex IV and ATP synthase subunit α (ATP5A) from complex V expression levels were analyzed by Western blotting in siControl and siANT2 cells at 48 and 96 hours post-transfection. It was only possible to quantify the protein levels of four of the five complexes since the signal of the subunit of Complex II was almost imperceptible (Fig. 11).

At 48 hours of transfection, a decrease of 30% in Complex I protein levels was observed, and Complex V tend to decrease in siANT2 cells ($p = 0.2337$) (Fig. 11A).

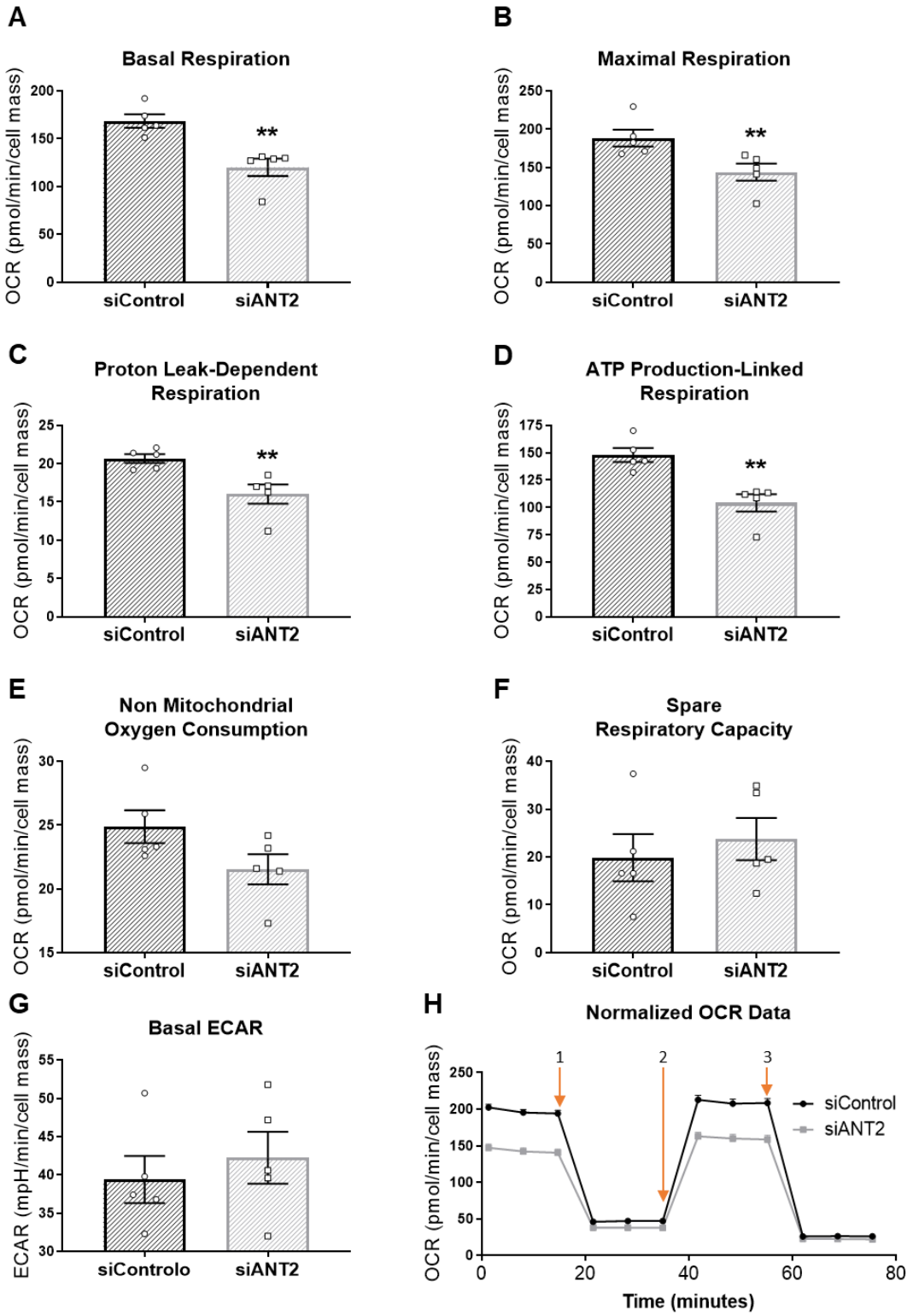

Figure 10 - Oxygen consumption rate parameters and basal extracellular acidification rate in siControl and siANT2 P19SCs. (A) Basal respiration, **(B)** Proton leak, **(C)** Maximal respiration, **(D)** Spare respiratory capacity, **(E)** Non-mitochondrial oxygen consumption, **(F)** ATP production, **(G)** Basal ECAR, and **(H)** OCR of 48 hours post-transfection P19SCs, with addition of 1) 3 µM oligomycin , 2) 0,25 µM FCCP and 3) 1 µM antimycin A and 1 µM rotenone. Data are presented as mean ± SEM of 4-6 replicates, from 5 independent experiments. Statistical analysis was performed using the non-parametric test Mann–Whitney. **: $p<0.01$.

The same tendency was observed for 96 hours of silencing (Fig. 11B). For complexes III and IV, it appears that there are no differences between siControl and siANT2 cells.

These data suggest that ANT2 silencing may promote mitochondrial remodeling and alteration in mitochondrial respiration.

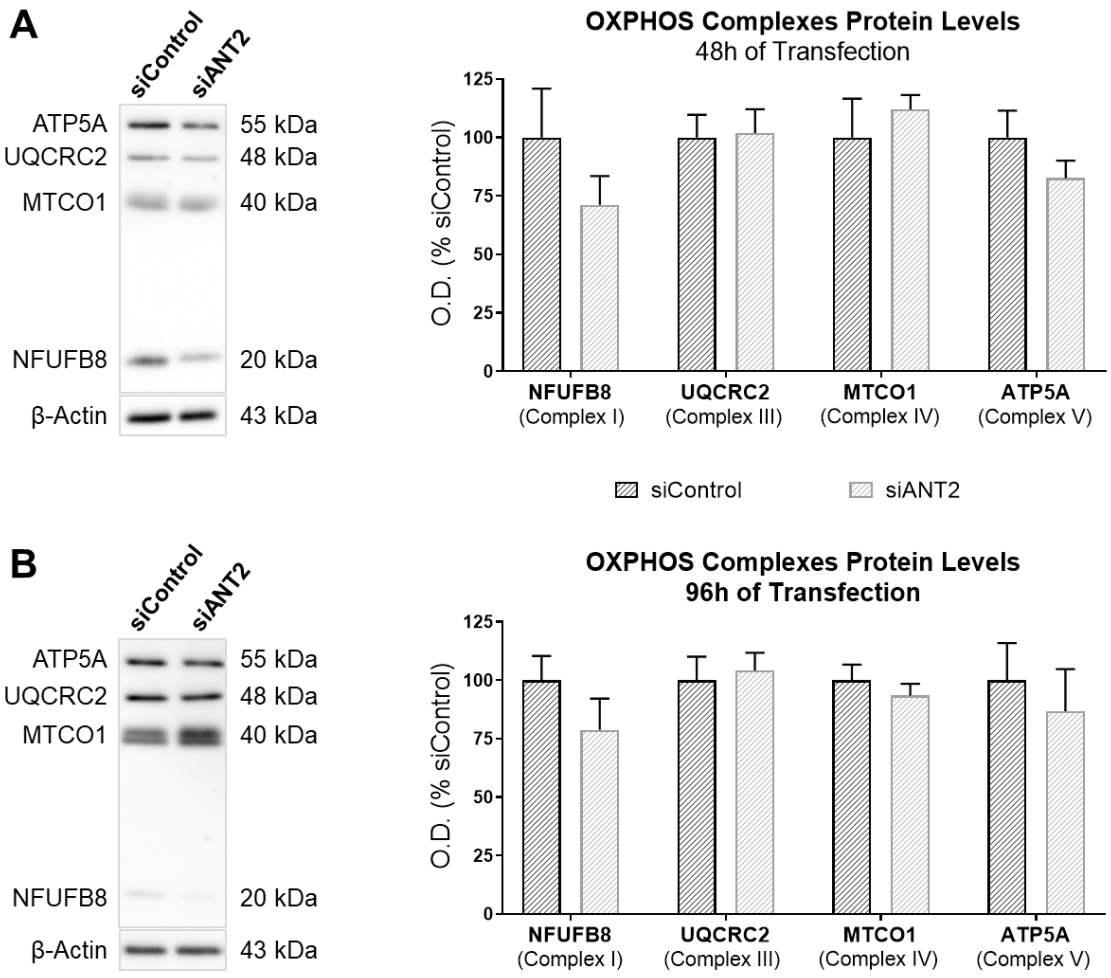

Figure 11 - OXPHOS complexes protein levels after transfection. **(A)** Representative Western blotting and respective protein expression levels of Complexes I, III, IV and V after 48h and **(B)** 96h of transfection. Data are presented as mean ± SEM expressed as percentage of siControl from, at least, 6 independent experiments. Statistical analysis was performed using Student's t test.

3.5. Mitochondrial potential decreased upon ANT2 silencing, but not the mitochondrial network area

Mitochondrial network area and mitochondrial membrane potential were assessed by confocal imaging, using Hoechst for nuclei labeling and TMRM dye for mitochondria labeling, after transfection. Representative images of siControl and siANT2 cells are shown in Figure 12A.

TMRM accumulates in negatively charge polarized mitochondria, so its intensity is proportional to mitochondrial membrane potential (125). As ANT2 plays a role in maintaining mitochondrial membrane potential, this parameter was evaluated by measuring TMRM intensity. To do so, different methods were used for better analysis and to understand what the most reliable approach. Furthermore, measurements were done in individual cells and in clusters of cells.

In order to evaluate if mitochondrial content was affected by ANT2 silencing, two different approaches were used: 1) measuring the area occupied by TMRM (Fig. 12A and G), and 2) addressing the percentage of each cell or cluster that was occupied by TMRM (Fig. 12B and H). No differences were found, with both conditions presenting similar mitochondrial network area. Regarding mitochondrial morphology, no analysis was done using this technique, so it was not possible to confirm if, in fact, mitochondrial dynamics was different in both conditions.

Mitochondrial membrane potential was also addressed in both cells and cluster of cells by measuring standard deviation (Fig. 12E and I) and mean gray value (Fig. 12F and J). It is possible to observe that siANT2 have decreased mitochondrial membrane potential when compared with siControl cells and cluster cells.

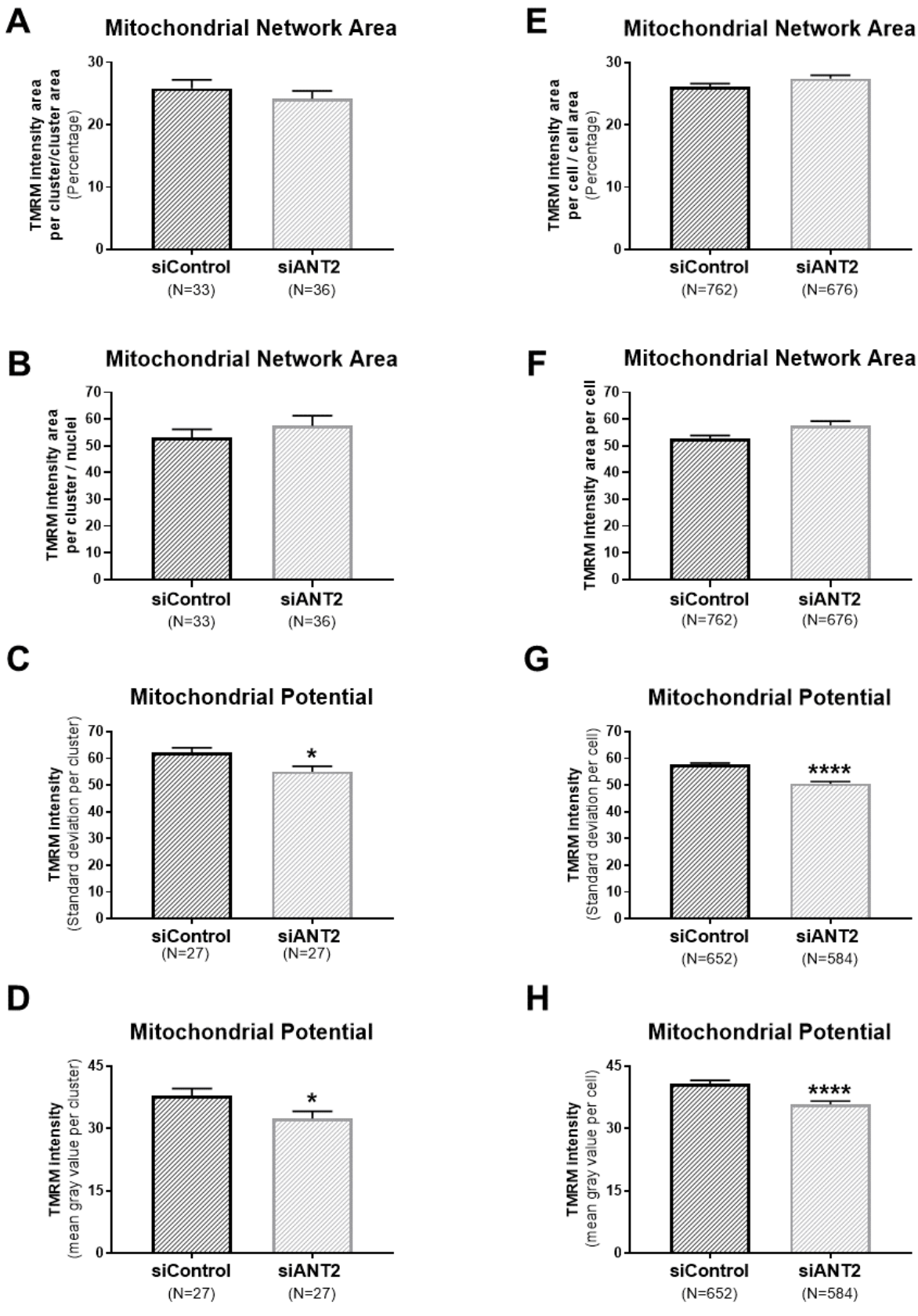
A
Mitochondrial Network Area
TMRM intensity area per cluster/cluster area (Percentage)
30
20
10
0
siControl
(N=33)
siANT2
(N=36)
E
Mitochondrial Network Area
TMRM intensity area per cell / cell area (Percentage)
30
20
10
0
siControl
(N=762)
siANT2
(N=676)
B
Mitochondrial Network Area
TMRM intensity area per cluster / nuclei
70
60
50
40
30
20
10
0
siControl
(N=33)
siANT2
(N=36)
F
Mitochondrial Network Area
TMRM intensity area per cell
70
60
50
40
30
20
10
0
siControl
(N=762)
siANT2
(N=676)
C
Mitochondrial Potential
TMRM Intensity (Standard deviation per cluster)
70
60
50
40
30
20
10
0
*
siControl
(N=27)
siANT2
(N=27)
G
Mitochondrial Potential
TMRM Intensity (Standard deviation per cell)
70
60
50
40
30
20
10
0
****
siControl
(N=652)
siANT2
(N=584)
D
Mitochondrial Potential
TMRM Intensity (mean gray value per cluster)
45
30
15
0
*
siControl
(N=27)
siANT2
(N=27)
H
Mitochondrial Potential
TMRM Intensity (mean gray value per cell)
45
30
15
0
****
siControl
(N=652)
siANT2
(N=584)

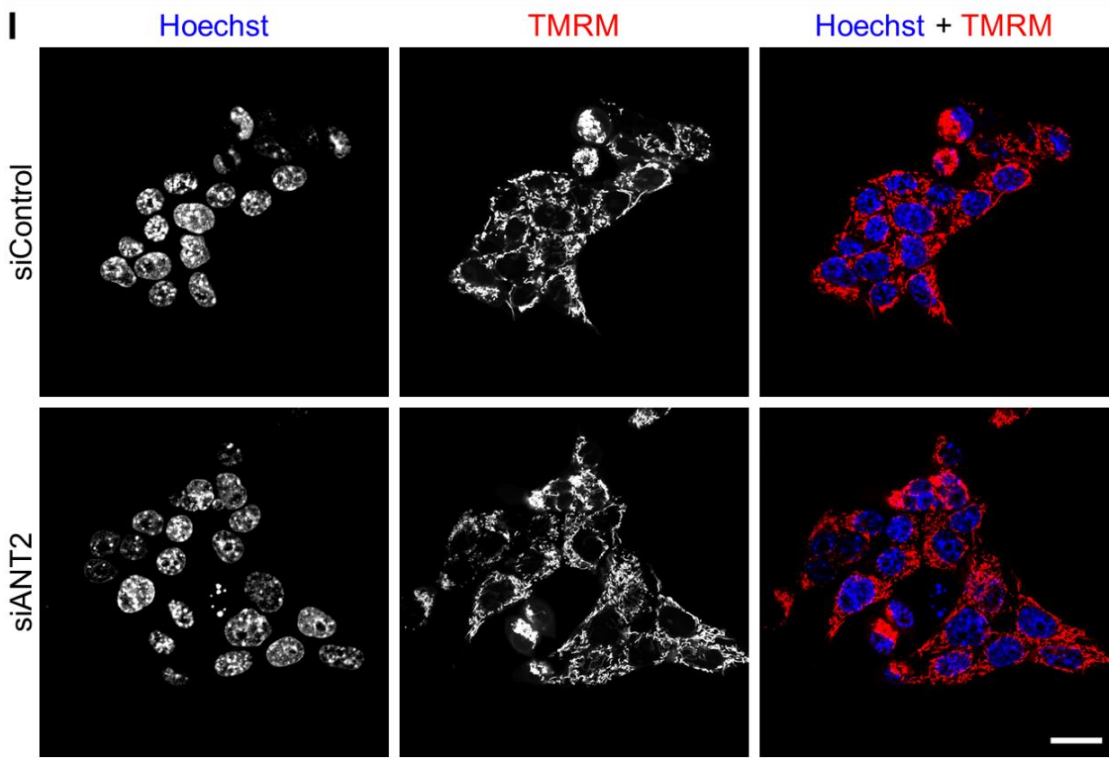

Figure 12 - Mitochondria from P19SCs after ANT2 silencing. (A)(B) Mitochondrial network area and **(C)(D)** mitochondrial membrane potential measured per cluster of cells. Data are expressed as mean ± SEM of 6 independent experiments. Statistical analysis was performed using Student's t-test. *: $p<0.05$; **(E)(F)** Mitochondrial network area and **(G)(H)** mitochondrial membrane potential measured per cell. Data are expressed as mean ± SEM of 6 independent experiments. Statistical analysis was performed using the non-parametric test Mann–Whitney. ****: $p<0,0001$. Number of cluster and cells analyzed are specified in each graph. (See section 2.2.10 for more details) **(I)** Representative confocal images of transfected cells obtained using TMRM and Hoechst for mitochondrial and nuclei labeling, respectively. Scale bar = 20μm.

3.6. Effect of ANT2 silencing on mitochondrial dynamics and biogenesis in P19 cells

In order to evaluate if ANT2 silencing affects mitochondrial dynamics, expression of proteins related to mitochondrial fission and fusion were analyzed. No differences were found in Mitofusin 1 (MFN1), a fusion protein, neither in Dynamin-related protein-1 (DRP1), a fission protein (Fig. 13A, B and F).

As these mitochondrial dynamics proteins seemed not to be affected, we next sought to investigate if mitochondrial biogenesis is impaired. To do so, peroxisome proliferator-activated receptor-gamma coactivator 1-alpha (PGC-1-

α), mitochondrial transcription factor A (TFAM), and translocase of outer membrane 20 (TOM20) expression levels were evaluated.

PGC-1-α is a transcription coactivator that, besides other functions, stimulates mitochondrial biogenesis (126). At 48 hours of transfection, expression levels of PGC-1-α decreased by 24% in siANT2 cells, comparing to siControl. However, no differences were found at 96 hours (Fig. 13C and F).

TFAM is involved in mtDNA transcription, replication, and maintenance (124). Thus, higher levels of TFAM are correlated with a higher rate of mitochondrial biogenesis. In ANT2 silenced cells, TFAM expression levels showed a tendency to decrease ($p = 0.2074$), having 30% less expression at 48 hours of transfection comparing to siControl cells. However, the same was not observed at 96 hours (Fig, 13D and F).

TOM20 levels of siANT2 cells were similar to siControl in both 48 and 96 hours, indicating that siControl and siANT2 cells have the same content of mitochondrial mass (Fig, 13E and F).

In summary, ANT2 silencing seems to not interfere with mitochondrial dynamics, since MFN1 and DRP1 expression levels were similar in both groups. But it does seem to play a role in mitochondrial biogenesis, at least in a short-term, since PGC-1-α and TFAM were slightly decreased (24 and 29%, respectively). However, TOM20 was not affected.

3.7. ANT2 silencing induced changes in P19 Cells metabolic-related enzymes

Based on the previous data, we wanted to analyze if expression levels of metabolic-related enzymes in P19 cells were affected by ANT2 silencing.

Hexokinase II (HKII) is the enzyme responsible for the conversion of Glucose to Glucose-6-Phosphate, the first reaction of glycolysis. Thus, protein levels

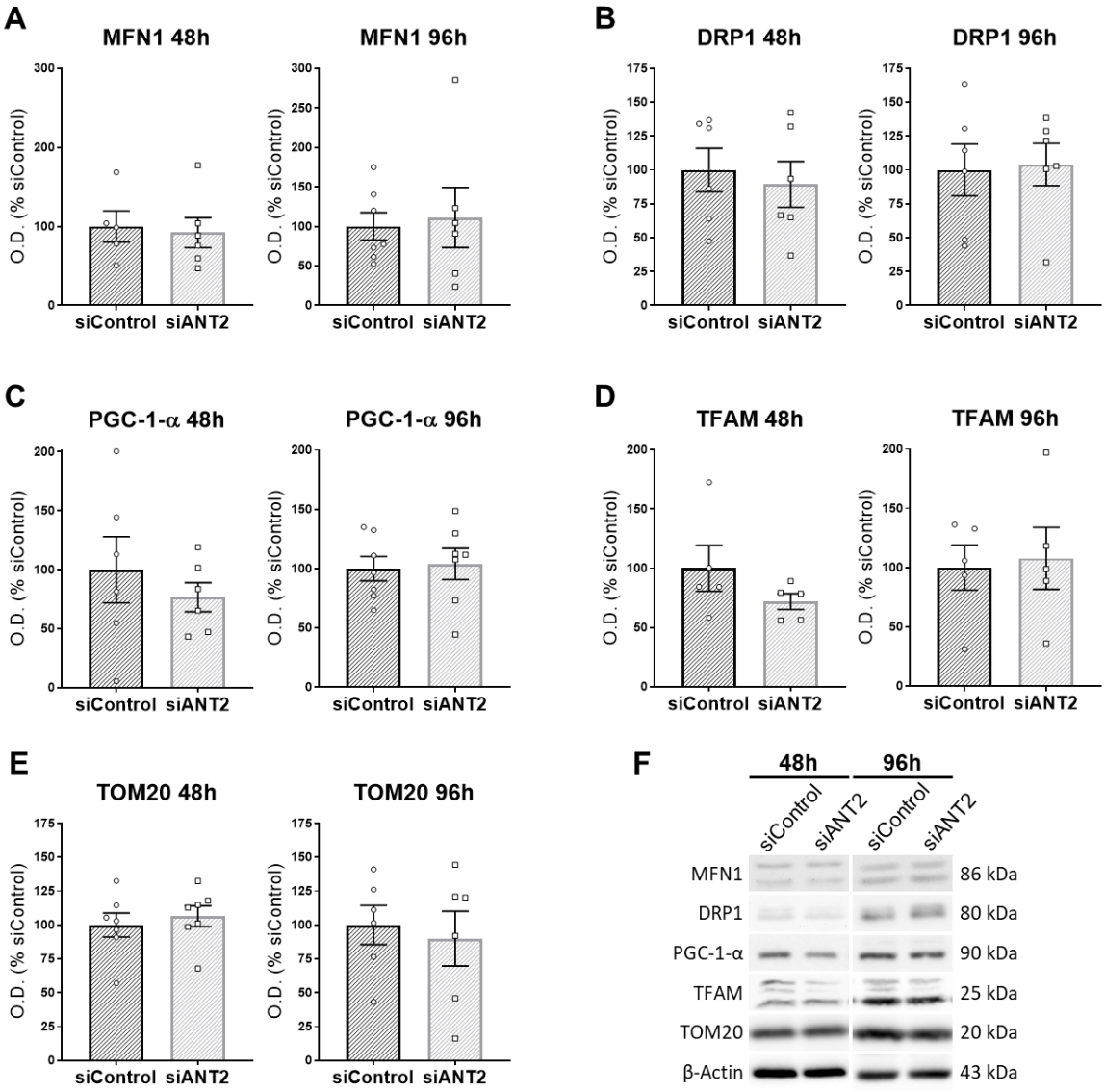

Figure 13 - Protein expression levels of mitochondrial dynamics and biogenesis-related proteins. **(A)** Mitofusin 1 (MFN1) and **(B)** Dynamin-related protein-1 (DRP1), proteins related to mitochondrial biogenesis, at 48 and 96 hours of transfection. **(C)** Peroxisome proliferator-activated receptor-gamma coactivator 1-alpha (PGC-1-α), **(D)** mitochondrial transcription factor (TFAM) and **(E)** translocase of outer membrane 20 (TOM20) expression levels at 48 and 96 hours post-transfection. Data are presented as mean ± SEM expressed as percentage of siControl from, at least, 5 independent experiments. Statistical analysis was performed using Student's t test. **(F)** Representative Western blotting of the proteins mentioned previously. β-Action was used as a loading control and normalization purposes.

analysis was done in P19 transfected cells in order to verify if HKII expression was affected by ANT2 silencing. A significant decrease was observed in both time points, with silenced cells having 30% less expression than siControl at 48 hours of transfection ($p < 0.05$), and 20% less at 96 hours ($p < 0.05$, Fig. 14A and D).

Pyruvate kinase muscle isozyme M2 (PKM2) catalyzes the final step in

glycolysis, converting phosphoenolpyruvate in pyruvate and is also know that is overexpressed in cancer (127). ANT2 silenced cells showed no differences in PKM2 expression levels when compared to siControl cells (Fig. 14B and D).

Pyruvate Dehydrogenase Kinase (PDK) participates in the regulation of Pyruvate Dehydrogenase activity (responsible for the conversion of pyruvate in Acetyl-CoA), inactivating it by phosphorylation. Expression levels of PDK at 48 hours of transfection were significantly decreased ($p < 0.01$), having almost 50% less expression that siControl cells (Fig. 14C and D).

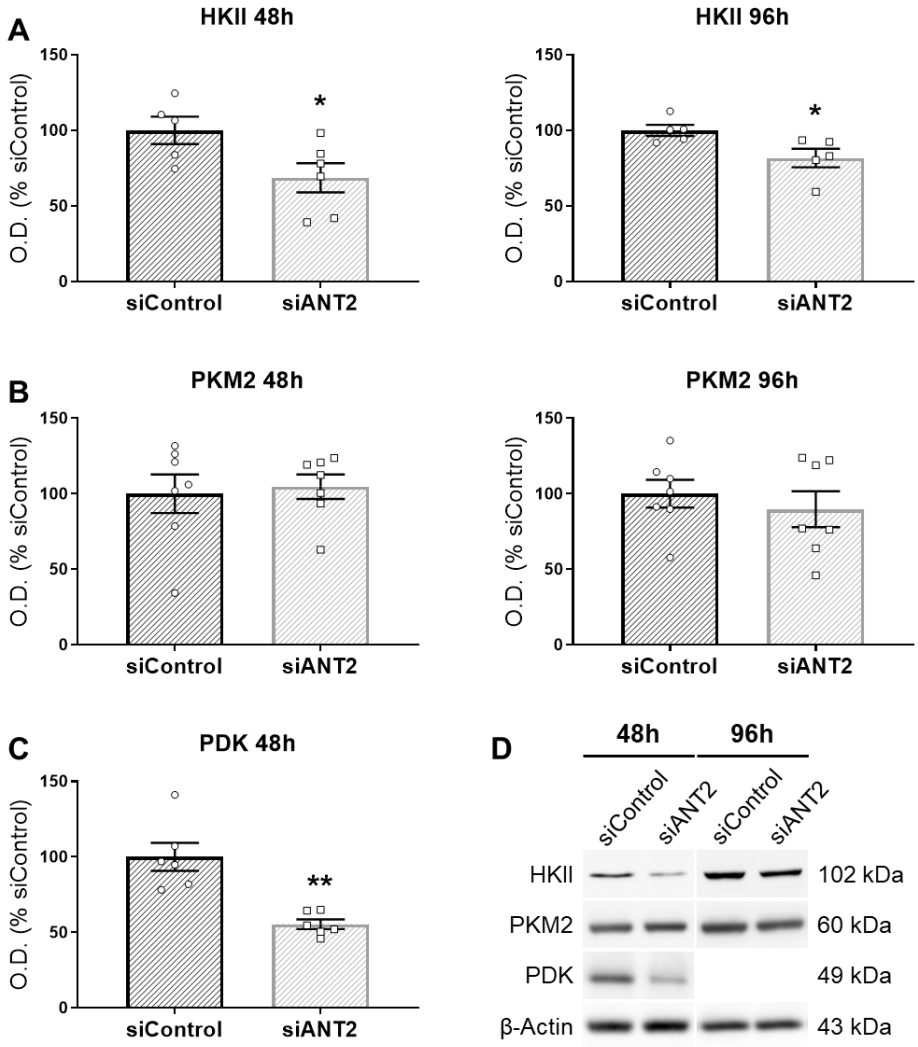

Figure 14 - Western blotting analyzes of enzymes related to cell metabolism. (A) Hexokinase II at 48 and 96 hours of transfection, **(B)** PKM2 after 48 and 96 hours of transfection, and **(C)** PDK at 48 hours of transfection. Data are presented as mean ± SEM expressed as percentage of siControl from, at least, 5 independent experiments. Statistical analysis was performed using Student's t-test. *: $p<0.05$; **: $p<0.01$ **(D)** Representative Western blotting of the proteins mentioned previously. Actin was used as a loading control and normalization purposes.

Thus, ANT2 silencing promotes a decrease in the expression levels of HKII and PDK, but PKM2 was not affected.

4. Discussion

Tumors are heterogeneous tissues composed of several cell types, which have different phenotypes, functions and states of differentiation (1, 2). Cancer stem cells (CSCs) are an example of cells that are present within a tumor and are known to have strong self-renewal properties, high tumorigenic and differentiation capacity, and are thought to be responsible for driving new tumors formation. Furthermore, CSCs are not targeted by conventional therapies, such as radio- and chemotherapy, and are believed to play a critical role in the onset of tumor relapse. All these characteristics confer to CSCs higher clinical potential and interest. Herein, we tried to contribute to a better understanding of the bases behind the abilities that these cells possess, with a particular emphasis on their metabolism. Several studies have shown that ANT2, a mitochondrial protein, is highly expressed in cancer cells, being associated with a glycolytic phenotype and high rates of proliferation (55, 128, 129). P19 carcinoma stem cells (P19SCs) were used in this work in order to study possible alterations in the mitochondrial profile of CSCs. As this cell line is easily differentiable into different fates, using it allowed us to study ANT expression in P19SCs and their differentiated counterparts, being our aim to find possible differences in ANT isoforms expression levels and how those isoforms influence CSCs metabolism. With this, we expect to obtain a better understanding of CSCs biology, as well as a possible starting point for the development of new target-strategies.

P19SCs exhibit a small and round shape, which is accompanied by a reduced expression of TROMA-I (marker for primitive endoderm) and β-3-Tubulin (marker for mature neurons), while OCT4 pluripotency marker is overexpressed. Upon treatment with retinoic acid, P19dCs lost OCT4 pluripotency marker, and TROMA-I (marker for primitive endoderm) and β-3-Tubulin (marker for mature neurons) expression levels were highly increased. Furthermore, an altered

morphology was also observed in P19dCs, with cells presenting a more elongated shape. In a previous study it was demonstrated that ANT1/2 levels were differently expressed in P19SCs relatively to their differentiated counterparts. However, the ANT isoform responsible for that difference was not completely clarified (86). As ANT2 silencing showed to induce apoptosis in cancer cells (112, 113), we aimed to uncover if ANT2 was overexpressed in P19SCs and deepen our knowledge about the role of this protein in CSCs and with a focus in mitochondrial biology. Here we confirmed that ANT1/2 expression was higher in P19dC, as described by Vega-Naredo et al. (86). Furthermore, we also demonstrate that, actually, ANT2 isoform is overexpressed in P19SCs, with P19dCs having less 73% of expression, which suggests that CSCs have a higher content of ANT2 than their differentiated counterparts. Our data are in agreement with several reports showing that ANT2 is overexpressed in proliferative cells (129, 130), undifferentiated cells (131), as well as in cancer cells (55, 112), including breast cancer stem cells (113).

In the present study we used ANT2-siRNA as a tool to inhibit ANT2 translation and we showed that, with this technique, we were able to diminish ANT2 levels up to 95%. The next step was to investigate if, with ANT2 silencing, P19 cells remain with stemness properties. Our results showed that ANT2 silencing was not sufficient to induce loss of stemness, with siANT2 cells having the same phenotype as P19SCs regarding cell morphology and pluripotency/differentiation markers.

ANT2 is a mitochondrial carrier protein that is thought to play an important role in the metabolic adaptation of cancer cells during tumorigenesis (55, 132), being also correlated with the aggressiveness of cancer cells (110). Moreover, it is known that Bcl2 family proteins modulate the activity of ANT isoforms (including ANT2) and ANT2 silencing in breast cancer and breast cancer-stem like cells diminished tumor growth and induced apoptosis (112, 113), suggesting ANT2 as an anti-apoptotic protein. Taking this into account, we sought to

investigate if ANT2 silencing affects cell growth in P19SCs. Cell mass and metabolic activity were measured after 24, 48, 72 and 96 hours of transfection. Albeit at 24 hours is already possible to see some effect, significant differences were only found after 48 and 72 hours of silencing when compared to siControl cells. Although no differences were found at 96 hours, it is not necessarily true that, at this timepoint, ANT2 silencing does not have an effect on both metabolic activity and cell mass. What could probably happen was that, as this cell line has rapid growth, they reached 100% confluency faster. So, siControl cells stopped proliferating because of the lack of space and, through time, siANT2 cells seemed to reach siControl levels. However, this could not mean that they have similar behaviors regarding these parameters. In spite of these, our data support that, at least for 48 and 72h hours of transfection, ANT2 silencing promotes a decrease in cell viability. Furthermore, the proliferative rate also seems to be decreased in siANT2 cells. Therefore, our data is in concordance with what is described in the literature for breast cancer cells and for breast cancer-stem like cells where ANT2 expression was depleted (112, 113).

ANT2 is specifically expressed in undifferentiated cells and its expression in cancer has been directly associated with glycolytic metabolism (55, 132). P19SCs are described as being glycolytic, relying on this pathway for energy supply (86). Glycolytic cancer cells import ATP produced via glycolysis into mitochondria through ANT2. This process is important for maintaining mitochondrial membrane potential, since ATP is used for pumping protons out of the matrix by F_1F_o-ATPase working in reverse mode (55, 115). As we observed a decreased in metabolic activity in silenced cells, we wondered if ANT2 silence could be promoting a metabolic shift and, possibly, OXPHOS could be altered. Mitochondrial function was measured and, interestingly, we found out that ANT2 silencing promotes a decrease in basal respiration, proton leak, maximal respiration and ATP production-linked respiration, which was accompanied by a slight decrease on subunits of Complex I and V protein levels, indicative that

they are less oxidative when compared to siControl cells. Mitochondrial content was assessed by TOM20 expression levels and by confocal imaging, by labeling mitochondria with TMRM. For analyzing mitochondrial network area, two different methods were also done. Firstly, by thresholding the images obtained by confocal microscopy, it was possible to calculate the area that is occupied by TMRM within the selection, which is proportional to mitochondrial network area. For cluster of cells, these number was normalized by nuclei number. Then, we also convert this area measurement in percentage, in order to observe the percentage of cell/cluster that is occupied by mitochondria. None of these parameters showed differences when comparing siANT2 cells to siControl cells, neither TOM20 expression. Taken together, these results suggest that different content of mitochondria is not the cause of the reduced OXPHOS observed in siANT2 cells.

It is thought that ANT2 is responsible for translocating ATP into mitochondria under some conditions. Therefore with ANT2 silencing, ATP uptake into the mitochondria could be compromised and, in that sense, also the maintenance of the mitochondrial membrane potential. Thus, as F_1F_o-ATPase probably will have less ATP to pumps protons out of the matrix, mitochondrial potential will possibly decrease, which can cause a lower efficiency on OXPHOS respiration. To test this hypothesis, mitochondrial potential was assessed in ANT2 silenced cells and clusters of cells using mean gray value and standard deviation. The mean gray value is calculated by summing the gray values of all the pixels and dividing it by the number of pixels, within the selection. Thus, this measurement tells us the average gray value of the area selected. Standard deviation measures the dispersion of the mean gray values relative to its mean, thus, low standard deviation means that the mean gray values are closed to the average, and high standard deviation tells us that the mean gray values are more spread out. In this particular context, standard deviation works as an indirect way of observing the differences between mitochondrial (TMRM) and cytosolic

labeling. By only measuring the mean gray value, possible variations would be lost, which, in this specific case, would be important in order to verify if mitochondria were more hyper- or depolarized. Therefore, both measurements were analyzed in order to better understand what is happening with mitochondrial membrane potential, and to have a more reliable analysis. Both types of analysis showed a decrease in ANT2 silenced cells and clusters, when compared to siControl. Thus, ANT2 silencing seems to induce a decrease in mitochondrial membrane potential, promoting a mitochondrial depolarization. The same was observed in breast cancer cells by Jang et. al (112), after ANT2 being silenced using shRNA. It was described by some authors that even a small decrease in this parameter might have a significant effect on energy homeostasis, since phosphorylation state of the ATP pool in the cytosol has high sensitiveness to minor alterations in mitochondrial membrane potential (133, 134, 135). In other words, a small depolarization of mitochondrial potential is sufficient to affect ATP production (136). Since siANT2 cells have a decrease of approximately 12-14% when compared to siControl cells (see supplementary data, Figure S1), this further might explain why OXPHOS is diminished. Furthermore, Jang et. al (112) also demonstrated that ANT2 knockdown in breast cancer cell promoted a significant reduction on intracellular ATP levels. However, although with no statistical differences, we also observed a decrease of 30% on protein levels of NDUFB8 subunit from Complex I at 48 hours of silencing. Thus, a decrease in complex I could also be the reason why OXPHOS is decreased, since less protein levels of Complex I could also mean less protons being pumped out of the mitochondrial matrix. Thus, in the future, the study of Complex I activity might be useful to better understand what could be happening.

Mitochondrial dynamics is known to be correlated with the metabolic needs of the cell, being fusion associated with more active mitochondria, and fission the opposite (137). As no analysis of mitochondrial morphology was done using confocal microscopy, we addressed this question by analyzing expression levels

of proteins related to mitochondrial dynamics and biogenesis. Cells where ANT2 was silenced shown no differences in fusion and fission processes, since MFN1 and DRP1 expression levels, respectively, were similar to control cells. Thus, these results suggest that ANT2 silencing does not have an effect on mitochondrial morphology. Mitochondrial biogenesis consists in the growth and division of pre-existing mitochondria (138, 139), being accompanied by alteration in mitochondrial size, mass and number (140). Its role in cancer is regulated by several factors, such as metabolic state, tissue type, tumor heterogeneity, among others (47). It is induced by PGC-1-α, and we show here that a slight decrease of 25% in its expression levels was detected after 48 hours of ANT2 silencing, when compared to siControl cells. It is described that this co-transcriptional regulation factor is often associated with mitochondrial respiration (47) and, as we demonstrate previously, siControl have a higher reliance on OXPHOS than siANT2 cells. In order to promote mitochondrial biogenesis, PGC-1-α activates different transcription factors that ultimately will promote the expression of TFAM (138, 141), which is responsible for mtDNA transcription, replication, and maintenance (124). TFAM levels were also decreased in ANT2 silenced cells, by 30%, after 48 hours of transfection. This raised the question whether mtDNA copy numbers were also affected, so in the future it might also be interesting to address this. As explained previously, mitochondrial biomass was not affected by ANT2 silencing, which is not in concordance with the decrease in mitochondrial biogenesis suggested by PGC-1-α and TFAM diminishing. However, mitophagy is also a central key in maintaining energy metabolism homeostasis (139), so a balance between mitochondrial biogenesis and mitophagy is needed (142, 143). One possible explanation for the fact that siANT2 cells have the same mitochondrial mass but slightly decreased markers of mitochondrial biogenesis could be a decrease in mitophagy fluxes. However, as mitophagy was not addressed in this work, we cannot confirm this hypothesis.

Facing these results and knowing that ANT2 is overexpressed in glycolytic cancer cells, we next sought to investigate cellular metabolic enzymes in order to understand what could be happening. PKM2, the enzyme responsible for catalyzing the final step of glycolysis, was not altered in silenced cells. However, some evidence showed that PKM2 might not have a rate-limiting effect on glycolysis (144). It is true that cancer cells have overexpression of this enzyme (127, 145, 146), but when silenced in different cell lines of cancer cells, glucose consumption and lactate generation did not decrease significantly (144). Furthermore, these levels also remained unchanged upon treatment with PKM2 activator (144). Altogether, these suggest that although PKM2 levels were not altered in ANT2 silenced cells, does not necessarily mean that the rate of glycolysis is similar to siControl cells. HKII expression levels, the enzyme responsible for the first reaction of glycolysis, were also evaluated. A significant decrease of 30% was found in siANT2 cells, when compared to siControl ones. It was described that HKII is able to bind to mitochondria by directly interacting with VDAC, which seems important for stabilizing a closed mPTP conformation (147). Furthermore, it was demonstrated that dissociation of HKII from mitochondria could cause cell death by apoptosis, but did not cause alteration on OXPHOS either on mitochondrial potential by itself (148). Thus, these pieces of evidence suggest that HKII has a dual role in cancer: 1) induces an increase in the glycolytic rate, catalyzing a rate-limiting step in this metabolic pathway (144), and 2) its association with mitochondria seems to inhibit apoptosis, by stabilizing a closed mPTP conformation (147, 148). Some authors also suggest that HKII bound to VDAC works reversely, using cytosolic glucose-6-phosphate to produce ATP, which is then uptake by ANT2 into mitochondria (55, 149). Taking all these evidence into consideration, a decrease in HKII levels could be a synonym of decreased glycolytic rate, or increased mitochondrial-induced apoptosis, or both. In fact, Jang et. al (112) suggest that ANT2 shRNA induces changes in Bcl-2 family balance in mitochondrial membranes in breast cancer

cells, resulting in cell death by favoring a proapoptotic pore-forming status. As HKII and Bcl-2 family proteins are thought to be part of mPTP, possibly both can be altered and play a role in mitochondria-induced apoptosis. Since only total levels of HKII were assessed in this work, we cannot say for sure which of the HKII roles is affected. However, as we also observed a decrease in cell proliferation, our theory is that HKII diminished levels might be associated with HKII bounded to mitochondria, promoting cell death by apoptosis. Nevertheless, more studies need to be done in order to support this hypothesis. We next sought to investigate PDK and PDH expression levels, since they are also known to be altered in cancer (150, 151). Pyruvate is the final product of glucose and, when it goes to mitochondria, is converted to acetyl-CoA by PDH complex, allowing to enter the Krebs cycle. The activity of PDH is inhibited by PDK through phosphorylation, and PDK activity is regulated by the concentration of NADH and acetyl-CoA (152). It is described that P19SCs present an inactive PDH, which is in concordance with their reliance on glycolysis (86). After several non-succeeded attempts to study PDH in ANT2-silenced cells, it was only possible to analyze PDK expression levels. When ANT2 is absent, PDK levels were reduced by almost 50%. Although we did not measure activity directly, this suggests that pyruvate is being oxidized to acetyl-CoA instead of being converted to lactic acid. However, without total and phosphorylated PDH levels or activity measurements is not possible to know if this is happening or not.

In sum, ANT2 silenced cells present a decreased cell proliferation when compared to cells transfected with negative control siRNA, which is accompanied by a decreased reliance on OXPHOS and decreased mitochondrial membrane potential. Mitochondrial mass and dynamics seem not to be affected, but mitochondrial biogenesis appears to be decreased in siANT2 cells. Altogether, these findings suggest that ANT2 silencing promotes a metabolic remodeling on P19SCs towards a less oxidative phenotype.

5. Conclusion

Growing evidence support that cancer stem cells (CSCs) are key drivers of tumor progression (63). CSCs are characterized by potent self-renewal and survival properties, being thought to be responsible for tumor recurrence, since they are not targeted by conventional therapies (62, 153). Moreover, they also demonstrate unique metabolic flexibility, which allows them to survive even under conditions of stress (154). Thus, a better understanding of this particular type of cancer cells to uncover their underlying mechanisms is still needed, since is crucial to identify possible targets to properly eliminate CSCs and overcome tumor relapse. Thereby, in this work we focused on ANT2, a mitochondrial protein that is known to be correlated with cancer metabolism. We hypothesized that silencing this protein could promote a metabolic remodeling in CSCs. As previous studies have suggested that ANT2 could be overexpressed in P19 embryonal carcinoma stem cells (86), we used this cell line as CSCs model to address this question.

Our findings show that ANT2 is indeed overexpressed in P19SCs when compared to their differentiated counterparts. Moreover, silencing ANT2 does not promote differentiation, indicating that this mitochondrial protein is not involved in the acquisition of stem-like phenotype. Accordingly to what was described by Jang et. al (113) in a breast stem-like cancer cell line, we also demonstrate that ANT2 knockdown induces cell proliferation arrest and possibly cell death. Furthermore, it induces a decreased on oxygen consumption and mitochondrial membrane potential, suggesting that silencing ANT2 promotes a remodeling towards a less oxidative metabolism, with some evidence that they might have a reduced glycolytic flux.

Based on our data and on the increasing evidence that ANT2 plays a role in the metabolic remodeling of CSCs, ANT2 could be a promising metabolic target for anticancer therapy of CSCs. Nevertheless, since normal proliferating cells

(such as kidney and liver cells) also express high levels of this mitochondrial protein (55), possible adverse effects should be taken into account.

6. Future Perspectives

To further investigations regarding the role of ANT2 in the metabolic remodeling of P19SCSs, the following experiments will be useful to be performed:

- Complex I activity, to further understand if diminished NDUFB8 subunit from Complex I protein levels is accompanied by a decrease on Complex I activity.
- Evaluate expression levels of both cytosolic and mitochondrial hexokinase II by Western blotting, to verify which of them is decreased in silenced cells.
- Cellular ATP levels will be addressed, in order to verify if silencing ANT2 in P19SCs promotes a decrease on these levels.
- Seahorse XF Glycolysis Stress Test, in order to unveil if glycolysis is also affected by the absence of ANT2.
- Mitochondrial permeability transition pore opening/induction by calcein/cobalt method, to verify if the decrease observed in cell mass and metabolic activity is due to mitochondria-induced apoptosis.
- Analysis of mitochondrial DNA (mtDNA), with the objective of knowing if ANT2 silencing promotes a decrease in mitochondrial biogenesis.
- Evaluate the chemosensitivity of siANT2 cells when exposed to chemotherapeutic agents, such as doxorubicin and cisplatin, by SRB and resazurin assays.

7. References

1. Hanahan D & Weinberg A. R. Hallmarks of Cancer: The Next Generation. *Cell* 2011 **144** 646–674. (doi:10.1016/j.cell.2011.02.013)
2. Hanahan D & Weinberg RA. The Hallmarks of Cancer. *Cell* 2000 **100** 57–70. (doi:10.1016/S0092-8674(00)81683-9)
3. Wieman HL, Wofford JA, & Rathmell JC. Cytokine stimulation promotes glucose uptake via phosphatidylinositol-3 kinase/Akt regulation of Glut1 activity and trafficking. *Molecular biology of the cell* 2007 **18** 1437–1446. (doi:10.1091/mbc.e06-07-0593)
4. Elstrom RL, Bauer DE, Buzzai M, Karnauskas R, Harris MH, Plas DR, Zhuang H, Cinalli RM, Alavi A, Rudin CM, & Thompson CB. Akt stimulates aerobic glycolysis in cancer cells. *Cancer research* 2004 **64** 3892–3899. (doi:10.1158/0008-5472.CAN-03-2904)
5. DeBerardinis RJ, Lum JJ, Hatzivassiliou G, & Thompson CB. The biology of cancer: metabolic reprogramming fuels cell growth and proliferation. *Cell metabolism* 2008 **7** 11–20. (doi:10.1016/j.cmet.2007.10.002)
6. Dzbek J & Korzeniewski B. Control over the contribution of the mitochondrial membrane potential (ΔΨ) and proton gradient (ΔpH) to the protonmotive force (Δp). *The Journal of biological chemistry* 2008 **283** 33232–33239. (doi:10.1074/jbc.M802404200)
7. Heiden MG Vander, Cantley LC, & Thompson CB. Understanding the Warburg effect: the metabolic requirements of cell proliferation. *Science (New York, N.Y.)* 2009 **324** 1029–1033. (doi:10.1126/science.1160809)
8. Warburg O. The Metabolism of Carcinoma Cells. *The Journal of Cancer Research* 1925 **9** 148–163. (doi:10.1158/jcr.1925.148)
9. Warburg O, Wind F, & Negelein E. The metabolism of tumors in the body. *The Journal of general physiology* 1927 **8** 519–530. (doi:10.1085/jgp.8.6.519)
10. Warburg O. On the origin of cancer cells. *Science (New York, N.Y.)* 1956 **123** 309–314. (doi:10.1126/science.123.3191.309)
11. Loos JA & Roos D. Changes in the carbohydrate metabolism of mitogenically stimulated human peripheral lymphocytes. 3. Stimulation by tuberculin and allogenic cells. *Experimental cell research* 1973 **79** 136–142. (doi:10.1016/0014-4827(73)90561-2)
12. Wang T, Marquardt C, & Foker J. Aerobic glycolysis during lymphocyte proliferation. *Nature* 1976 **261** 702–705. (doi:10.1038/261702a0)
13. Fantin VR, St-Pierre J, & Leder P. Attenuation of LDH-A expression uncovers a link between glycolysis, mitochondrial physiology, and tumor maintenance. *Cancer cell* 2006 **9** 425–434. (doi:10.1016/j.ccr.2006.04.023)
14. Moreno-Sánchez R, Rodríguez-Enríquez S, Marín-Hernández A, & Saavedra E.

Energy metabolism in tumor cells. *The FEBS journal* 2007 **274** 1393–1418. (doi:10.1111/j.1742-4658.2007.05686.x)

15. Gatenby RA & Gillies RJ. Why do cancers have high aerobic glycolysis? *Nature Reviews Cancer* 2004 **4** 891–899. (doi:10.1038/nrc1478)
16. Pfeiffer T, Schuster S, & Bonhoeffer S. Cooperation and competition in the evolution of ATP-producing pathways. *Science (New York, N.Y.)* 2001 **292** 504–507. (doi:10.1126/science.1058079)
17. Mazurek S, Boschek CB, Hugo F, & Eigenbrodt E. Pyruvate kinase type M2 and its role in tumor growth and spreading. *Seminars in cancer biology* 2005 **15** 300–308. (doi:10.1016/j.semcancer.2005.04.009)
18. Mathupala SP, Ko YH, & Pedersen PL. Hexokinase-2 bound to mitochondria: cancer's stygian link to the 'Warburg Effect' and a pivotal target for effective therapy. *Seminars in cancer biology* 2009 **19** 17–24. (doi:10.1016/j.semcancer.2008.11.006)
19. Ganapathy V, Thangaraju M, & Prasad PD. Nutrient transporters in cancer: relevance to Warburg hypothesis and beyond. *Pharmacology & therapeutics* 2009 **121** 29–40. (doi:10.1016/j.pharmthera.2008.09.005)
20. Jóźwiak P, Forma E, Bryś M, & Krześlak A. O-GlcNAcylation and metabolic reprograming in cancer. *Frontiers in endocrinology* 2014 **5** 145. (doi:10.3389/fendo.2014.00145)
21. Fang J, Quinones QJ, Holman TL, Morowitz MJ, Wang Q, Zhao H, Sivo F, Maris JM, & Wahl ML. The H+-linked monocarboxylate transporter (MCT1/SLC16A1): a potential therapeutic target for high-risk neuroblastoma. *Molecular pharmacology* 2006 **70** 2108–2115. (doi:10.1124/mol.106.026245)
22. Pinheiro C, Longatto-Filho A, Scapulatempo C, Ferreira L, Martins S, Pellerin L, Rodrigues M, Alves VAF, Schmitt F, & Baltazar F. Increased expression of monocarboxylate transporters 1, 2, and 4 in colorectal carcinomas. *Virchows Archiv : an international journal of pathology* 2008 **452** 139–146. (doi:10.1007/s00428-007-0558-5)
23. Stern R, Shuster S, Neudecker BA, & Formby B. Lactate stimulates fibroblast expression of hyaluronan and CD44: the Warburg effect revisited. *Experimental cell research* 2002 **276** 24–31. (doi:10.1006/excr.2002.5508)
24. Robey IF, Baggett BK, Kirkpatrick ND, Roe DJ, Dosescu J, Sloane BF, Hashim AI, Morse DL, Raghunand N, Gatenby RA, & Gillies RJ. Bicarbonate Increases Tumor pH and Inhibits Spontaneous Metastases. *Cancer research* 2009 **69** 2260–2268. (doi:10.1158/0008-5472.CAN-07-5575)
25. San-Millán I & Brooks GA. Reexamining cancer metabolism: lactate production for carcinogenesis could be the purpose and explanation of the Warburg Effect. *Carcinogenesis* 2017 **38** 119–133. (doi:10.1093/carcin/bgw127)
26. Bellance N, Lestienne P, & Rossignol R. Mitochondria: from bioenergetics to the metabolic regulation of carcinogenesis. *Frontiers in bioscience (Landmark edition)*

2009 **14** 4015–4034.

27. Phan LM, Yeung SCJ, & Lee MH. Cancer metabolic reprogramming: importance, main features, and potentials for precise targeted anti-cancer therapies. *Cancer biology & medicine* 2014 **11** 1–19. (doi:10.7497/j.issn.2095-3941.2014.01.001)
28. Jiang P, Du W, & Wu M. Regulation of the pentose phosphate pathway in cancer. *Protein & Cell* 2014 **5** 592–602. (doi:10.1007/s13238-014-0082-8)
29. Riganti C, Gazzano E, Polimeni M, Aldieri E, & Ghigo D. The pentose phosphate pathway: an antioxidant defense and a crossroad in tumor cell fate. *Free radical biology & medicine* 2012 **53** 421–436. (doi:10.1016/j.freeradbiomed.2012.05.006)
30. Deberardinis RJ, Sayed N, Ditsworth D, & Thompson CB. Brick by brick: metabolism and tumor cell growth. *Current opinion in genetics & development* 2008 **18** 54–61. (doi:10.1016/j.gde.2008.02.003)
31. DeBerardinis RJ, Mancuso A, Daikhin E, Nissim I, Yudkoff M, Wehrli S, & Thompson CB. Beyond aerobic glycolysis: Transformed cells can engage in glutamine metabolism that exceeds the requirement for protein and nucleotide synthesis. *Proceedings of the National Academy of Sciences* 2007 **104** 19345–19350. (doi:10.1073/pnas.0709747104)
32. Iurlaro R, León-Annicchiarico CL, & Muñoz-Pinedo C. Regulation of cancer metabolism by oncogenes and tumor suppressors. *Methods in enzymology* 2014 **542** 59–80. (doi:10.1016/B978-0-12-416618-9.00003-0)
33. Cantley LC. The phosphoinositide 3-kinase pathway. *Science (New York, N.Y.)* 2002 **296** 1655–1657. (doi:10.1126/science.296.5573.1655)
34. Samuels Y, Diaz LA, Schmidt-Kittler O, Cummins JM, Delong L, Cheong I, Rago C, Huso DL, Lengauer C, Kinzler KW, Vogelstein B, & Velculescu VE. Mutant PIK3CA promotes cell growth and invasion of human cancer cells. *Cancer cell* 2005 **7** 561–573. (doi:10.1016/j.ccr.2005.05.014)
35. Elstrom RL, Bauer DE, Buzzai M, Karnauskas R, Harris MH, Plas DR, Zhuang H, Cinalli RM, Alavi A, Rudin CM, & Thompson CB. Akt stimulates aerobic glycolysis in cancer cells. *Cancer research* 2004 **64** 3892–3899. (doi:10.1158/0008-5472.CAN-03-2904)
36. Engelman JA, Luo J, & Cantley LC. The evolution of phosphatidylinositol 3-kinases as regulators of growth and metabolism. *Nature reviews. Genetics* 2006 **7** 606–619. (doi:10.1038/nrg1879)
37. Manning BD & Cantley LC. AKT/PKB signaling: navigating downstream. *Cell* 2007 **129** 1261–1274. (doi:10.1016/j.cell.2007.06.009)
38. Cairns RA. Drivers of the Warburg phenotype. *Cancer journal (Sudbury, Mass.)* 2015 **21** 56–61. (doi:10.1097/PPO.0000000000000106)
39. Semenza GL. HIF-1: upstream and downstream of cancer metabolism. *Current opinion in genetics & development* 2010 **20** 51–56. (doi:10.1016/j.gde.2009.10.009)
40. Dang C V., Kim J whan, Gao P, & Yustein J. The interplay between MYC and HIF in cancer. *Nature reviews cancer* 2008 **8** 51–56. (doi:10.1038/nrc2274)

41. Gao P, Tchernyshyov I, Chang TC, Lee YS, Kita K, Ochi T, Zeller KI, Marzo AM De, Eyk JE Van, Mendell JT, & Dang C V. c-Myc suppression of miR-23a/b enhances mitochondrial glutaminase expression and glutamine metabolism. *Nature* 2009 **458** 762–765. (doi:10.1038/nature07823)
42. Vousden KH & Ryan KM. p53 and metabolism. *Nature Reviews Cancer* 2009 **9** 691–700. (doi:10.1038/nrc2715)
43. Bensaad K, Tsuruta A, Selak MA, Vidal MNC, Nakano K, Bartrons R, Gottlieb E, & Vousden KH. TIGAR, a p53-inducible regulator of glycolysis and apoptosis. *Cell* 2006 **126** 107–120. (doi:10.1016/j.cell.2006.05.036)
44. Barbosa IA, Machado NG, Skildum AJ, Scott PM, & Oliveira PJ. Mitochondrial remodeling in cancer metabolism and survival: potential for new therapies. *Biochimica et biophysica acta* 2012 **1826** 238–254. (doi:10.1016/j.bbcan.2012.04.005)
45. Gottlieb E & Tomlinson IPM. Mitochondrial tumour suppressors: a genetic and biochemical update. *Nature Reviews Cancer* 2005 **5** 857–866. (doi:10.1038/nrc1737)
46. King A, Selak MA, & Gottlieb E. Succinate dehydrogenase and fumarate hydratase: linking mitochondrial dysfunction and cancer. *Oncogene* 2006 **25** 4675–4682. (doi:10.1038/sj.onc.1209594)
47. Vyas S, Zaganjor E, & Haigis MC. Mitochondria and cancer. *Cell* 2016 **166** 555–566. (doi:10.1016/j.cell.2016.07.002)
48. Kasahara A & Scorrano L. Mitochondria: from cell death executioners to regulators of cell differentiation. *Trends in cell biology* 2014 **24** 761–770. (doi:10.1016/j.tcb.2014.08.005)
49. Mishra P & Chan DC. Metabolic regulation of mitochondrial dynamics. *The Journal of cell biology* 2016 **212** 379–387. (doi:10.1083/jcb.201511036)
50. Liesa M, Palacín M, & Zorzano A. Mitochondrial dynamics in mammalian health and disease. *Physiological reviews* 2009 **89** 799–845. (doi:10.1152/physrev.00030.2008)
51. Wallace DC. Mitochondria and cancer. *Nature reviews. Cancer* 2012 **12** 685–698. (doi:10.1038/nrc3365)
52. Senft D & Ronai ZA. Regulators of mitochondrial dynamics in cancer. *Current opinion in cell biology* 2016 **39** 43–52. (doi:10.1016/j.ceb.2016.02.001)
53. Rehman J, Zhang HJ, Toth PT, Zhang Y, Marsboom G, Hong Z, Salgia R, Husain AN, Wietholt C, & Archer SL. Inhibition of mitochondrial fission prevents cell cycle progression in lung cancer. *FASEB journal : official publication of the Federation of American Societies for Experimental Biology* 2012 **26** 2175–2186. (doi:10.1096/fj.11-196543)
54. Zhao J, Zhang J, Yu M, Xie Y, Huang Y, Wolff DW, Abel PW, & Tu Y. Mitochondrial dynamics regulates migration and invasion of breast cancer cells. *Oncogene* 2013 **32** 4814–4824. (doi:10.1038/onc.2012.494)
55. Chevrollier A, Loiseau D, Reynier P, & Stepien G. Adenine nucleotide translocase 2 is a key mitochondrial protein in cancer metabolism. *Biochimica et Biophysica Acta*

(BBA) - Bioenergetics 2011 **1807** 562–567. (doi:10.1016/j.bbabio.2010.10.008)

56. Bhat TA, Kumar S, Chaudhary AK, Yadav N, & Chandra D. Restoration of mitochondria function as a target for cancer therapy. *Drug discovery today* 2015 **20** 635–643. (doi:10.1016/j.drudis.2015.03.001)
57. Brunelle JK & Letai A. Control of mitochondrial apoptosis by the Bcl-2 family. *Journal of cell science* 2009 **122** 437–441. (doi:10.1242/jcs.031682)
58. Zamzami N & Kroemer G. The mitochondrion in apoptosis: how Pandora's box opens. *Nature Reviews Molecular Cell Biology* 2001 **2** 67–71. (doi:10.1038/35048073)
59. Forrest MD. Why cancer cells have a more hyperpolarised mitochondrial membrane potential and emergent prospects for therapy. *bioRxiv* 2015 1–42. (doi:10.1101/025197)
60. Carew JS & Huang P. Mitochondrial defects in cancer. *Molecular cancer* 2002 **1** 9. (doi:10.1186/1476-4598-1-9)
61. Chandra D & Singh KK. Genetic insights into OXPHOS defect and its role in cancer. *Biochimica et biophysica acta* 2011 **1807** 620–625. (doi:10.1016/j.bbabio.2010.10.023)
62. Pietras A. Cancer stem cells in tumor heterogeneity. *Advances in cancer research* 2011 **112** 255–281. (doi:10.1016/B978-0-12-387688-1.00009-0)
63. Jordan CT, Guzman ML, & Noble M. Cancer stem cells. *The New England journal of medicine* 2006 **355** 1253–1261. (doi:10.1056/NEJMra061808)
64. Meacham CE & Morrison SJ. Tumour heterogeneity and cancer cell plasticity. *Nature* 2013 **501** 328–337. (doi:10.1038/nature12624)
65. Bonnet D & Dick JE. Human acute myeloid leukemia is organized as a hierarchy that originates from a primitive hematopoietic cell. *Nature medicine* 1997 **3** 730–737. (doi:10.1038/nm0797-730)
66. Michor F & Polyak K. The origins and implications of intratumor heterogeneity. *Cancer prevention research (Philadelphia, Pa.)* 2010 **3** 1361–1364. (doi:10.1158/1940-6207.CAPR-10-0234)
67. Barabé F, Kennedy JA, Hope KJ, & Dick JE. Modeling the initiation and progression of human acute leukemia in mice. *Science (New York, N.Y.)* 2007 **316** 600–604. (doi:10.1126/science.1139851)
68. Lapidot T, Sirard C, Vormoor J, Murdoch B, Hoang T, Caceres-Cortes J, Minden M, Paterson B, Caligiuri MA, & Dick JE. A cell initiating human acute myeloid leukaemia after transplantation into SCID mice. *Nature* 1994 **367** 645–648. (doi:10.1038/367645a0)
69. Al-Hajj M, Wicha MS, Benito-Hernandez A, Morrison SJ, & Clarke MF. Prospective identification of tumorigenic breast cancer cells. 2003 **100** . (doi:10.1073/pnas.1131491100)
70. Singh SK, Hawkins C, Clarke ID, Squire JA, Bayani J, Hide T, Henkelman RM, Cusimano MD, & Dirks PB. Identification of human brain tumour initiating cells. *Nature* 2004 **432** 396–401. (doi:10.1038/nature03128)

71. Ricci-Vitiani L, Lombardi DG, Pilozzi E, Biffoni M, Todaro M, Peschle C, & Maria R De. Identification and expansion of human colon-cancer-initiating cells. *Nature* 2007 **445** 111–115. (doi:10.1038/nature05384)
72. Li C, Heidt DG, Dalerba P, Burant CF, Zhang L, Adsay V, Wicha M, Clarke MF, & Simeone DM. Identification of pancreatic cancer stem cells. *Cancer research* 2007 **67** 1030–1037. (doi:10.1158/0008-5472.CAN-06-2030)
73. Bjerkvig R, Tysnes BB, Aboody KS, Najbauer J, & Terzis AJA. Opinion: the origin of the cancer stem cell: current controversies and new insights. *Nature reviews. Cancer* 2005 **5** 899–904. (doi:10.1038/nrc1740)
74. Clarke MF, Dick JE, Dirks PB, Eaves CJ, Jamieson CHM, Jones DL, Visvader J, Weissman IL, & Wahl GM. Cancer stem cells--perspectives on current status and future directions: AACR Workshop on cancer stem cells. *Cancer research* 2006 **66** 9339–9344. (doi:10.1158/0008-5472.CAN-06-3126)
75. Jang H, Yang J, Lee E, & Cheong JH. Metabolism in embryonic and cancer stemness. *Archives of pharmacal research* 2015 **38** 381–388. (doi:10.1007/s12272-015-0558-y)
76. Kurtova A V., Xiao J, Mo Q, Pazhanisamy S, Krasnow R, Lerner SP, Chen F, Roh TT, Lay E, Ho PL, & Chan KS. Blocking PGE2-induced tumour repopulation abrogates bladder cancer chemoresistance. *Nature* 2015 **517** 209–213. (doi:10.1038/nature14034)
77. Safa AR. Resistance to Cell Death and Its Modulation in Cancer Stem Cells. *Critical Reviews™ in Oncogenesis* 2016 **21** 203–219. (doi:10.1615/CritRevOncog.2016016976)
78. Maugeri-Saccà M, Bartucci M, & Maria R De. DNA damage repair pathways in cancer stem cells. *Molecular cancer therapeutics* 2012 **11** 1627–1636. (doi:10.1158/1535-7163.MCT-11-1040)
79. Begicevic RR & Falasca M. ABC Transporters in Cancer Stem Cells: Beyond Chemoresistance. *International journal of molecular sciences* 2017 **18** 2362. (doi:10.3390/ijms18112362)
80. Fletcher JI, Haber M, Henderson MJ, & Norris MD. ABC transporters in cancer: more than just drug efflux pumps. *Nature reviews. Cancer* 2010 **10** 147–156. (doi:10.1038/nrc2789)
81. Fletcher JI, Williams RT, Henderson MJ, Norris MD, & Haber M. ABC transporters as mediators of drug resistance and contributors to cancer cell biology. *Drug Resistance Updates* 2016 **26** 1–9. (doi:10.1016/j.drup.2016.03.001)
82. Samuels Y, Diaz LA, Schmidt-Kittler O, Cummins JM, Delong L, Cheong I, Rago C, Huso DL, Lengauer C, Kinzler KW, Vogelstein B, & Velculescu VE. Mutant PIK3CA promotes cell growth and invasion of human cancer cells. *Cancer cell* 2005 **7** 561–573. (doi:10.1016/j.ccr.2005.05.014)
83. Yuan S, Lu Y, Yang J, Chen G, Kim S, Feng L, Ogasawara M, Hammoudi N, Lu W, Zhang H, Liu J, Colman H, Lee JS, Li XN, Xu R hua, Huang P, & Wang F. Metabolic activation of mitochondria in glioma stem cells promotes cancer

development through a reactive oxygen species-mediated mechanism. *Stem cell research & therapy* 2015 **6** 198. (doi:10.1186/s13287-015-0174-2)

84. Snyder V, Reed-Newman TC, Arnold L, Thomas SM, & Anant S. Cancer Stem Cell Metabolism and Potential Therapeutic Targets. *Frontiers in Oncology* 2018 **8** 203. (doi:10.3389/fonc.2018.00203)
85. Peiris-Pagès M, Martinez-Outschoorn UE, Pestell RG, Sotgia F, & Lisanti MP. Cancer stem cell metabolism. *Breast Cancer Research* 2016 **18** 55. (doi:10.1186/s13058-016-0712-6)
86. Vega-Naredo I, Loureiro R, Mesquita KA, Barbosa IA, Tavares LC, Branco AF, Erickson JR, Holy J, Perkins EL, Carvalho RA, & Oliveira PJ. Mitochondrial metabolism directs stemness and differentiation in P19 embryonal carcinoma stem cells. *Cell Death & Differentiation* 2014 **21** 1560–1574. (doi:10.1038/cdd.2014.66)
87. Yuen CA, Asuthkar S, Guda MR, Tsung AJ, & Velpula KK. Cancer stem cell molecular reprogramming of the Warburg effect in glioblastomas: a new target gleaned from an old concept. *CNS oncology* 2016 **5** 101–108. (doi:10.2217/cns-2015-0006)
88. Palorini R, Votta G, Balestrieri C, Monestiroli A, Olivieri S, Vento R, & Chiaradonna F. Energy metabolism characterization of a novel cancer stem cell-like line 3AB-OS. *Journal of cellular biochemistry* 2014 **115** 368–379. (doi:10.1002/jcb.24671)
89. Kondoh H, Lleonart ME, Gil J, Wang J, Degan P, Peters G, Martinez D, Carnero A, & Beach D. Glycolytic enzymes can modulate cellular life span. *Cancer research* 2005 **65** 177–185.
90. Pastò A, Bellio C, Pilotto G, Ciminale V, Silic-Benussi M, Guzzo G, Rasola A, Frasson C, Nardo G, Zulato E, Nicoletto MO, Manicone M, Indraccolo S, & Amadori A. Cancer stem cells from epithelial ovarian cancer patients privilege oxidative phosphorylation, and resist glucose deprivation. *Oncotarget* 2014 **5** 4305–4319. (doi:10.18632/oncotarget.2010)
91. Prigione A, Fauler B, Lurz R, Lehrach H, & Adjaye J. The senescence-related mitochondrial/oxidative stress pathway is repressed in human induced pluripotent stem cells. *Stem cells (Dayton, Ohio)* 2010 **28** 721–733. (doi:10.1002/stem.404)
92. Loureiro R, Mesquita KA, Magalhães-Novais S, Oliveira PJ, & Vega-Naredo I. Mitochondrial biology in cancer stem cells. *Seminars in cancer biology* 2017 **47** 18–28. (doi:10.1016/j.semcancer.2017.06.012)
93. Peiris-Pagès M, Bonuccelli G, Sotgia F, & Lisanti MP. Mitochondrial fission as a driver of stemness in tumor cells: mDIVI1 inhibits mitochondrial function, cell migration and cancer stem cell (CSC) signalling. *Oncotarget* 2018 **9** 13254–13275. (doi:10.18632/oncotarget.24285)
94. Xie Q, Wu Q, Horbinski CM, Flavahan WA, Yang K, Zhou W, Dombrowski SM, Huang Z, Fang X, Shi Y, Ferguson AN, Kashatus DF, Bao S, & Rich JN.

Mitochondrial control by DRP1 in brain tumor initiating cells. *Nature neuroscience* 2015 **18** 501–510. (doi:10.1038/nn.3960)

95. Vazquez F, Lim JH, Chim H, Bhalla K, Girnun G, Pierce K, Clish CB, Granter SR, Widlund HR, Spiegelman BM, & Puigserver P. PGC1α expression defines a subset of human melanoma tumors with increased mitochondrial capacity and resistance to oxidative stress. *Cancer cell* 2013 **23** 287–301. (doi:10.1016/j.ccr.2012.11.020)
96. LeBleu VS, O'Connell JT, Gonzalez Herrera KN, Wikman H, Pantel K, Haigis MC, Carvalho FM de, Damascena A, Domingos Chinen LT, Rocha RM, Asara JM, & Kalluri R. PGC-1α mediates mitochondrial biogenesis and oxidative phosphorylation in cancer cells to promote metastasis. *Nature cell biology* 2014 **16** 992–1003, 1–15. (doi:10.1038/ncb3039)
97. Luca A De, Fiorillo M, Peiris-Pagès M, Ozsvari B, Smith DL, Sanchez-Alvarez R, Martinez-Outschoorn UE, Cappello AR, Pezzi V, Lisanti MP, & Sotgia F. Mitochondrial biogenesis is required for the anchorage-independent survival and propagation of stem-like cancer cells. *Oncotarget* 2015 **6** 14777–14795. (doi:10.18632/oncotarget.4401)
98. Peiris-Pagès M, Martinez-Outschoorn UE, Pestell RG, Sotgia F, & Lisanti MP. Cancer stem cell metabolism. *Breast cancer research : BCR* 2016 **18** 55. (doi:10.1186/s13058-016-0712-6)
99. Ciavardelli D, Rossi C, Barcaroli D, Volpe S, Consalvo A, Zucchelli M, Cola A De, Scavo E, Carollo R, D'Agostino D, Forlì F, D'Aguanno S, Todaro M, Stassi G, Ilio C Di, Laurenzi V De, & Urbani A. Breast cancer stem cells rely on fermentative glycolysis and are sensitive to 2-deoxyglucose treatment. *Cell death & disease* 2014 **5** e1336. (doi:10.1038/cddis.2014.285)
100. Liu Y & Chen XJ. Adenine nucleotide translocase, mitochondrial stress, and degenerative cell death. *Oxidative medicine and cellular longevity* 2013 **2013** . (doi:10.1155/2013/146860)
101. Halestrap AP & Brenner C. The adenine nucleotide translocase: a central component of the mitochondrial permeability transition pore and key player in cell death. *Current medicinal chemistry* 2003 **10** 1507–1525. (doi:10.2174/0929867033457278)
102. Maldonado EN, DeHart DN, Patnaik J, Klatt SC, Gooz MB, & Lemasters JJ. ATP/ADP Turnover and import of glycolytic ATP into mitochondria in cancer cells is independent of the adenine nucleotide translocator. *The Journal of biological chemistry* 2016 **291** 19642–19650. (doi:10.1074/jbc.M116.734814)
103. Cao G, Minami M, Pei W, Yan C, Chen D, O'Horo C, Graham SH, & Chen J. Intracellular Bax translocation after transient cerebral ischemia: implications for a role of the mitochondrial apoptotic signaling pathway in ischemic neuronal death. *Journal of cerebral blood flow and metabolism : official journal of the International Society of Cerebral Blood Flow and Metabolism* 2001 **21** 321–333. (doi:10.1097/00004647-

200104000-00001)

104. Crompton M. The mitochondrial permeability transition pore and its role in cell death. *The Biochemical journal* 1999 **341 (Pt 2** 233–249. (doi:10.1007/s10495-007-0723-y)

105. Woodfield K, Rück A, Brdiczka D, & Halestrap AP. Direct demonstration of a specific interaction between cyclophilin-D and the adenine nucleotide translocase confirms their role in the mitochondrial permeability transition. *The Biochemical journal* 1998 **336 (Pt 2)** 287–290. (doi:10.1042/bj3360287)

106. Crompton M, Virji S, & Ward JM. Cyclophilin-D binds strongly to complexes of the voltage-dependent anion channel and the adenine nucleotide translocase to form the permeability transition pore. *European journal of biochemistry* 1998 **258** 729–735. (doi:10.1046/j.1432-1327.1998.2580729.x)

107. Kokoszka JE, Waymire KG, Levy SE, Sligh JE, Cai J, Jones DP, MacGregor GR, & Wallace DC. The ADP/ATP translocator is not essential for the mitochondrial permeability transition pore. *Nature* 2004 **427** 461–465. (doi:10.1038/nature02229)

108. Brenner C, Subramaniam K, Pertuiset C, & Pervaiz S. Adenine nucleotide translocase family: four isoforms for apoptosis modulation in cancer. *Oncogene* 2011 **30** 883–895. (doi:10.1038/onc.2010.501)

109. Sharaf el dein O, Mayola E, Chopineau J, & Brenner C. The adenine nucleotide translocase 2, a mitochondrial target for anticancer biotherapy. *Current drug targets* 2011 **12** 894–901. (doi:BSP/CDT/E-Pub/00234 [pii])

110. Chevrollier A, Loiseau D, Chabi B, Renier G, Douay O, Malthièry Y, & Stepien G. ANT2 isoform required for cancer cell glycolysis. *Journal of bioenergetics and biomembranes* 2005 **37** 307–316. (doi:10.1007/s10863-005-8642-5)

111. Bras M Le, Borgne-Sanchez A, Touat Z, Dein OS El, Deniaud A, Maillier E, Lecellier G, Rebouillat D, Lemaire C, Kroemer G, Jacotot E, & Brenner C. Chemosensitization by Knockdown of Adenine Nucleotide Translocase-2. *Cancer Research* 2006 **66** 9143–9152. (doi:10.1158/0008-5472.CAN-05-4407)

112. Jang JY, Choi Y, Jeon YK, & Kim CW. Suppression of adenine nucleotide translocase-2 by vector-based siRNA in human breast cancer cells induces apoptosis and inhibits tumor growth in vitro and in vivo. *Breast Cancer Research* 2008 **10** R11. (doi:10.1186/bcr1857)

113. Jang JY, Kim MK, Jeon YK, Joung YK, Park KD, & Kim CW. Adenovirus adenine nucleotide translocator-2 shRNA effectively induces apoptosis and enhances chemosensitivity by the down-regulation of ABCG2 in breast cancer stem-like cells. *Experimental and Molecular Medicine* 2012 **44** 251–259. (doi:10.3858/emm.2012.44.4.019)

114. Loiseau D, Chevrollier A, Douay O, Vavasseur F, Renier G, Reynier P, Malthièry Y, & Stepien G. Oxygen consumption and expression of the adenine nucleotide translocator in cells lacking mitochondrial DNA. *Experimental cell research* 2002 **278** 12–18. (doi:10.1006/excr.2002.5553)

115. Garedew A, Henderson SO, & Moncada S. Activated macrophages utilize glycolytic ATP to maintain mitochondrial membrane potential and prevent apoptotic cell death. *Cell death and differentiation* 2010 **17** 1540–1550. (doi:10.1038/cdd.2010.27)
116. McBurney MW & Rogers BJ. Isolation of male embryonal carcinoma cells and their chromosome replication patterns. *Developmental biology* 1982 **89** 503–508. (doi:10.1016/0012-1606(82)90338-4)
117. McBurney MW. P19 embryonal carcinoma cells. *The International journal of developmental biology* 1993 **37** 135–140. (doi:8507558)
118. Hyun Baik S & Lee J. Adenine nucleotide translocase 2: an emerging player in cancer. *Journal of Stem Cell Research and Medicine* 2016 **1** 66–68. (doi:10.15761/JSCRM.1000111)
119. Kim TK & Eberwine JH. Mammalian cell transfection: the present and the future. *Analytical and bioanalytical chemistry* 2010 **397** 3173–3178. (doi:10.1007/s00216-010-3821-6)
120. O'Brien J, Wilson I, Orton T, & Pognan F. Investigation of the Alamar Blue (resazurin) fluorescent dye for the assessment of mammalian cell cytotoxicity. *European journal of biochemistry* 2000 **267** 5421–5426. (doi:10.1046/j.1432-1327.2000.01606.x)
121. Silva FSG, Starostina IG, Ivanova V V., Rizvanov AA, Oliveira PJ, & Pereira SP. Determination of Metabolic Viability and Cell Mass Using a Tandem Resazurin/Sulforhodamine B Assay. *Current Protocols in Toxicology* 2016 **68** 2.24.1-2.24.15. (doi:10.1002/cptx.1)
122. Papazisis KT, Geromichalos GD, Dimitriadis KA, & Kortsaris AH. Optimization of the sulforhodamine B colorimetric assay. *Journal of immunological methods* 1997 **208** 151–158. (doi:10.1016/s0022-1759(97)00137-3)
123. Vichai V & Kirtikara K. Sulforhodamine B colorimetric assay for cytotoxicity screening. *Nature Protocols* 2006 **1** 1112–1116. (doi:10.1038/nprot.2006.179)
124. Nirwane A & Majumdar A. Understanding mitochondrial biogenesis through energy sensing pathways and its translation in cardio-metabolic health. *Archives of Physiology and Biochemistry* 2018 **124** 194–206. (doi:10.1080/13813455.2017.1391847)
125. Scaduto RC & Grotyohann LW. Measurement of mitochondrial membrane potential using fluorescent rhodamine derivatives. *Biophysical journal* 1999 **76** 469–477. (doi:10.1016/S0006-3495(99)77214-0)
126. Liang H & Ward WF. PGC-1alpha: a key regulator of energy metabolism. *Advances in physiology education* 2006 **30** 145–151. (doi:10.1152/advan.00052.2006)
127. DONG G, MAO Q, XIA W, XU Y, WANG J, XU L, & JIANG F. PKM2 and cancer: The function of PKM2 beyond glycolysis. *Oncology Letters* 2016 **11** 1980–1986. (doi:10.3892/ol.2016.4168)
128. Giraud S, Bonod-Bidaud C, Wesolowski-Louvel M, & Stepien G. Expression of

human ANT2 gene in highly proliferative cells: GRBOX, a new transcriptional element, is involved in the regulation of glycolytic ATP import into mitochondria. *Journal of molecular biology* 1998 **281** 409–418. (doi:10.1006/jmbi.1998.1955)

129. Barath P, Luciakova K, Hodny Z, Li R, & Nelson BD. The growth-dependent expression of the adenine nucleotide translocase-2 (ANT2) gene is regulated at the level of transcription and is a marker of cell proliferation. *Experimental cell research* 1999 **248** 583–588. (doi:10.1006/excr.1999.4432)
130. Dolce V, Scarcia P, Iacopetta D, & Palmieri F. A fourth ADP/ATP carrier isoform in man: Identification, bacterial expression, functional characterization and tissue distribution. *FEBS Letters* 2005 **579** 633–637. (doi:10.1016/j.febslet.2004.12.034)
131. Stepien G, Torroni A, Chung AB, Hodge JA, & Wallaces DC. Differential expression of adenine nucleotide translocator isoforms in mammalian tissues and during muscle cell differentiation. *Journal of Biological Chemistry* 1992 **267** 14592–14597.
132. Hyun Baik S & Lee J. Adenine nucleotide translocase 2: an emerging player in cancer. *Journal of Stem Cell Research and Medicine* 2016 **1** . (doi:10.15761/JSCRM.1000111)
133. Nicholls DG. Mitochondrial membrane potential and aging. *Aging Cell* 2004 **3** 35–40. (doi:10.1111/j.1474-9728.2003.00079.x)
134. Distelmaier F, Koopman WJH, Testa ER, Jong AS de, Swarts HG, Mayatepek E, Smeitink JAM, & Willems PHGM. Life cell quantification of mitochondrial membrane potential at the single organelle level. *Cytometry. Part A : the journal of the International Society for Analytical Cytology* 2008 **73** 129–138. (doi:10.1002/cyto.a.20503)
135. Koopman WJH, Nijtmans LGJ, Dieteren CEJ, Roestenberg P, Valsecchi F, Smeitink JAM, & Willems PHGM. Mammalian mitochondrial complex I: biogenesis, regulation, and reactive oxygen species generation. *Antioxidants & redox signaling* 2010 **12** 1431–1470. (doi:10.1089/ars.2009.2743)
136. Distelmaier F, Koopman WJH, Heuvel LP van den, Rodenburg RJ, Mayatepek E, Willems PHGM, & Smeitink JAM. Mitochondrial complex I deficiency: from organelle dysfunction to clinical disease. *Brain* 2008 **132** 833–842. (doi:10.1093/brain/awp058)
137. Westermann B. Bioenergetic role of mitochondrial fusion and fission. *Biochimica et biophysica acta* 2012 **1817** 1833–1838. (doi:10.1016/j.bbabio.2012.02.033)
138. Jornayvaz FR & Shulman GI. Regulation of mitochondrial biogenesis. *Essays In Biochemistry* 2010 **47** 69–84. (doi:10.1042/bse0470069)
139. Palikaras K, Lionaki E, & Tavernarakis N. Balancing mitochondrial biogenesis and mitophagy to maintain energy metabolism homeostasis. *Cell death and differentiation* 2015 **22** 1399–1401. (doi:10.1038/cdd.2015.86)
140. Ventura-Clapier R, Garnier A, & Veksler V. Transcriptional control of mitochondrial biogenesis: the central role of PGC-1alpha. *Cardiovascular research*

2008 **79** 208–217. (doi:10.1093/cvr/cvn098)

141. Picca A & Lezza AMS. Regulation of mitochondrial biogenesis through TFAM-mitochondrial DNA interactions: Useful insights from aging and calorie restriction studies. *Mitochondrion* 2015 **25** 67–75. (doi:10.1016/j.mito.2015.10.001)
142. Zhu J, Wang KZQ, & Chu CT. After the banquet: mitochondrial biogenesis, mitophagy, and cell survival. *Autophagy* 2013 **9** 1663–1676. (doi:10.4161/auto.24135)
143. Bordi M, Nazio F, & Campello S. The close interconnection between mitochondrial dynamics and mitophagy in cancer. *Frontiers in oncology* 2017 **7** 81. (doi:10.3389/fonc.2017.00081)
144. Xie J, Dai C, & Hu X. Evidence That Does Not Support Pyruvate Kinase M2 (PKM2)-catalyzed Reaction as a Rate-limiting Step in Cancer Cell Glycolysis. *Journal of Biological Chemistry* 2016 **291** 8987–8999. (doi:10.1074/jbc.M115.704825)
145. Lim JY, Yoon SO, Seol SY, Hong SW, Kim JW, Choi SH, & Cho JY. Overexpression of the M2 isoform of pyruvate kinase is an adverse prognostic factor for signet ring cell gastric cancer. *World journal of gastroenterology* 2012 **18** 4037–4043. (doi:10.3748/wjg.v18.i30.4037)
146. Mohammad GH, Olde Damink SWM, Malago M, Dhar DK, & Pereira SP. Pyruvate Kinase M2 and Lactate Dehydrogenase A Are Overexpressed in Pancreatic Cancer and Correlate with Poor Outcome. *PloS one* 2016 **11** e0151635. (doi:10.1371/journal.pone.0151635)
147. Loureiro R, Mesquita KA, Oliveira PJ, & Vega-Naredo I. Mitochondria in cancer stem cells: a target for therapy. *Recent patents on endocrine, metabolic & immune drug discovery* 2013 **7** 102–114. (doi:10.2174/18722148113079990006)
148. Chen Z, Zhang H, Lu W, & Huang P. Role of mitochondria-associated hexokinase II in cancer cell death induced by 3-bromopyruvate. *Biochimica et biophysica acta* 2009 **1787** 553–560. (doi:10.1016/j.bbabio.2009.03.003)
149. Depaoli MR, Karsten F, Madreiter-Sokolowski CT, Klec C, Gottschalk B, Bischof H, Eroglu E, Waldeck-Weiermair M, Simmen T, Graier WF, & Malli R. Real-Time Imaging of Mitochondrial ATP Dynamics Reveals the Metabolic Setting of Single Cells. *Cell Reports* 2018 **25** 501-512.e3. (doi:10.1016/j.celrep.2018.09.027)
150. Koukourakis MI, Giatromanolaki A, Sivridis E, Gatter KC, Harris AL, & Tumor and Angiogenesis Research Group. Pyruvate dehydrogenase and pyruvate dehydrogenase kinase expression in non small cell lung cancer and tumor-associated stroma. *Neoplasia (New York, N.Y.)* 2005 **7** 1–6. (doi:10.1593/neo.04373)
151. Lu CW, Lin SC, Chien CW, Lin SC, Lee CT, Lin BW, Lee JC, & Tsai SJ. Overexpression of pyruvate dehydrogenase kinase 3 increases drug resistance and early recurrence in colon cancer. *The American journal of pathology* 2011 **179** 1405–1414. (doi:10.1016/j.ajpath.2011.05.050)
152. Shaw RJ. Glucose metabolism and cancer. *Current opinion in cell biology* 2006 **18** 598–608. (doi:10.1016/j.ceb.2006.10.005)

153. Adorno-Cruz V, Kibria G, Liu X, Doherty M, Junk DJ, Guan D, Hubert C, Venere M, Mulkearns-Hubert E, Sinyuk M, Alvarado A, Caplan AI, Rich J, Gerson SL, Lathia J, & Liu H. Cancer stem cells: targeting the roots of cancer, seeds of metastasis, and sources of therapy resistance. *Cancer research* 2015 **75** 924–929. (doi:10.1158/0008-5472.CAN-14-3225)
154. Sancho P, Barneda D, & Heeschen C. Hallmarks of cancer stem cell metabolism. *British Journal of Cancer* 2016 **114** 1305–1312. (doi:10.1038/bjc.2016.152)

8. Supplementary Data

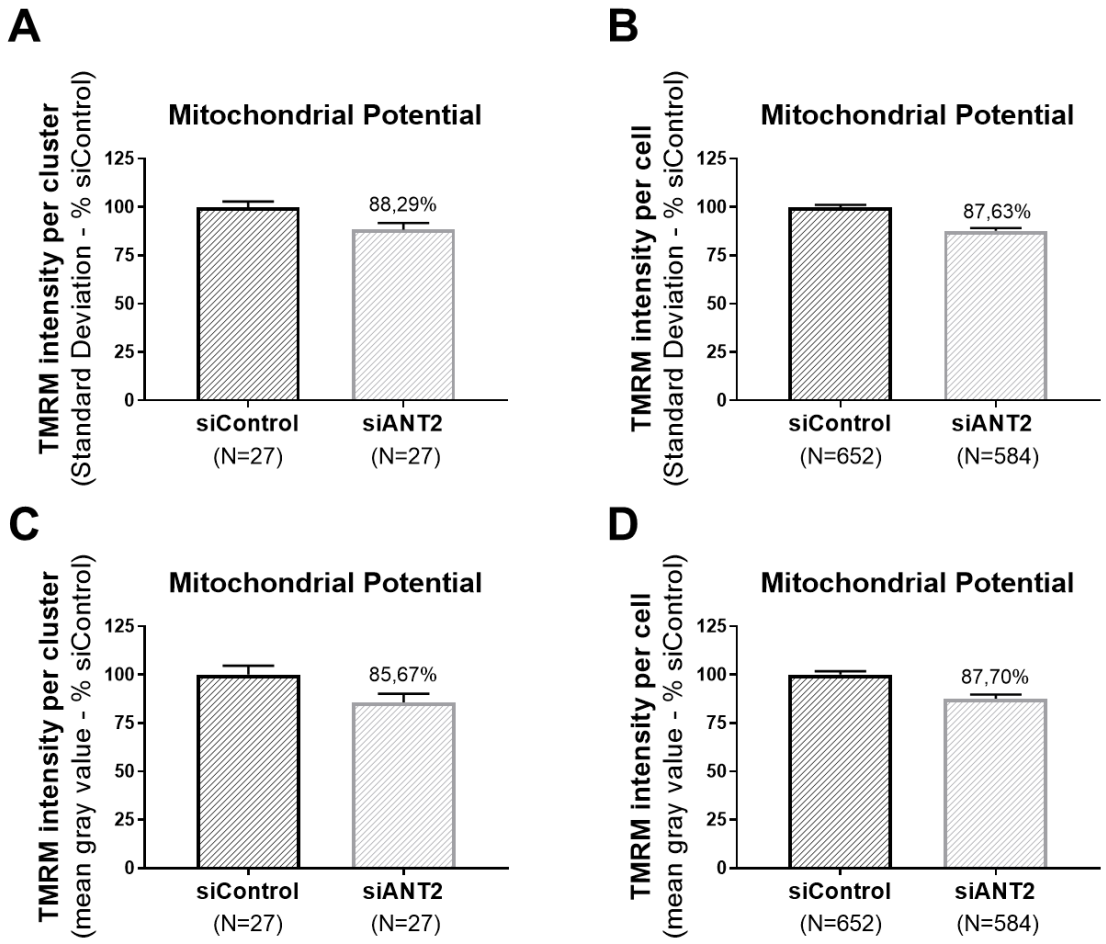

Figure S 1 - Mitochondrial membrane potential in P19 transfected cells by TMRM labeling. (A)(B) using standard deviation in clusters and cells, respectively; and **(C)(D)** by mean gray value in clusters and cells. Data are presented as mean ± SEM expressed as percentage of siControl cells. Number of cells analyzed are specified in each graph. (See section 2.2.10 for more details).